# PHOTOCURING EPOXY WITH QUANTUM DOTS FOR 3D PRINTING

Keroles B. Riad

A Thesis

in

The Individualized Program

Engineering

Presented in Partial Fulfillment of Requirements

for the Degree of the Master of Science at

Concordia University Montreal, Quebec, Canada

2015

February 2016

**CONCORDIA UNIVERSITY**

**School of Graduate Studies**

This is to certify that the thesis prepared

By: **Keroles Riad**

Entitled: **"Photocuring epoxy with quantum dots for 3D printing"** and submitted in partial fulfillment of the requirements for the degree of:

Masters of Science- INDI engineering

complies with the regulations of the University and meets the accepted standards with respect to originality and quality.

Signed by the final examining committee:

_____ Chair

Professor Charles Reiss

_____ Examiner

Professor Jerome Clavérie

_____ Examiner

Professor Rolf Wüthrich

_____ Supervisor

Professor Paula Wood-Adams

Approved by

_____

Chair of Department or Graduate Program Director

_____

Dean of Faculty

_____

Date

_____

# ABSTRACT

## Photocuring epoxy with quantum dots for 3D printing

**Keroles Riad**

3D printing is the future of manufacturing, limited by material development. Stereolithography is an ideal 3D printing process as it is energy efficient, accurate, fast and capable of forming composite materials. The photocuring of polymers used in this process is integral to society via more applications such as dentistry, coating, and printed circuit boards. However, those photosensitive materials are unstable in daylight during end use limiting their viability for making functional parts in many applications, motivating our work. The ultimate goal is to photocure only with light outside of the solar spectrum on Earth in stereolithography 3D printing, which motivates this work, to produce photostable parts.

While semiconducting nanoparticles have previously been shown to photocure acrylic resins via a free radical mechanism, here we demonstrate, for the first time, that semiconducting nanoparticles are capable of photocuring epoxy cationically. This result is critical because with that achieved, the quantized effect can be used to increase the band gap energy of the nanoparticles to only be sensitive to light outside of the solar spectrum on Earth.

We study both bulk and quantized nanoparticles, propose a reaction mechanism supported by experimental observations, and explore the effects of process variables on the kinetics of the reaction. The intertwining of the engineering of the application, the chemistry of the reactions and the physics of quantum dots makes this thesis a truly rich, interdisciplinary study.

## DEDICATION

I dedicate this thesis to my nurses and doctors in the medical day hospital in the new Glen hospital and the old Montreal children hospital; I owe them my life.

## ACKNOWLEDGMENT

I thank my supervisors: professors Wood-Adams, Claverie and Wurthich for their invaluable support, guidance, extreme patience and for making my research experience one of the most I have ever enjoyed. I thank Professor Hoa for allowing me to use his facilities. I also thank Concordia Institute of Aerospace Design and Innovation (CIADI) to whom I owe my career. I am grateful for my lab mates for their help and support. Last but not least, I am grateful to my family: Basem, Mervat, Gerges and little Philo for bearing with me and for their unconditional love.

## TABLE OF CONTENTS

**List of Figures**

# 1. Introduction

## Engineering

### Production process

Production is a multistep process to transform an idea to a product consisting of a closed loop of designing, modeling and manufacturing. Success is evaluated with the cost, time and quality triangle. Rapid prototyping is critical to modeling but rarely used in manufacturing.[1]

Prototyping is modeling a design either via a physical or a virtual model. Physical prototyping is expensive and time consuming but provides good feedback to the iterative process. Virtual prototyping uses computer aided software that models and tests designs. Virtual prototyping saves cost and time while supplying accurate feedback but it cannot replace some necessary physical tests. Modeling is, thus, crucial for testing and optimization.[2]

Manufacturing transforms raw material into a product. A manufacturing process is either formative, subtractive or additive. Formative manufacturing plastically deforms raw material into the desired shape as in bending and rolling. Subtractive manufacturing removes pieces out of a block of raw material to reach the desired shape. Milling and drilling are two such processes. Additive manufacturing adds material to reach the desired shape. Welding and 3D printing are examples of such processes. 3D printing is the focus of this thesis.[2]

### 3D printing

3D printing is similar to printing on paper where ink is deposited on the paper line by line and a picture is formed as those lines stack up. In 3D printing, thin layers of material, corresponding to the cross-section of the parts, are formed on a platform and stacked one on top of the other to form a 3D part as outlined in Figure 1.1.[2]

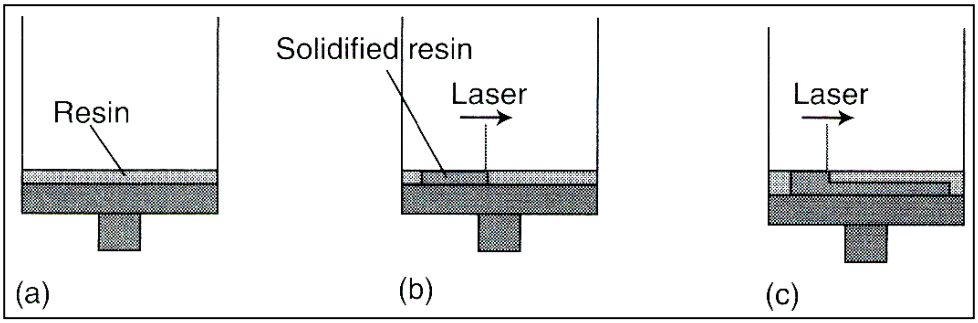


*Figure 1-1:* ***An outline of a 3D printing process.*** *a) The process starts with a layer of liquid material. b) A laser traces in XY plane to solidify a cross-section. c) The platform moves down, another layer of liquid is swept on top of previous layer and another cross-section is solidified.*[2]

There are many 3D printing processes: fusion deposition modeling (FDM) (Figure 1.2), selective laser sintering (SLS) (Figure 1.3) and stereolithography (SLA) (Figure 1.4). FDM uses materials with a low melting temperature like thermoplastic filaments of PLA or ABS which are extruded through a heater that melts the plastic and deposits it on a platform to form a layer of material. Then, the extruder moves up and deposits another layer on top of the previous one and so on until a 3D part is built.[2] In SLS, the entire printing chamber is sealed and heated up to a temperature right below the melting point of the powder. A powerful laser is used to locally heat the powder above its melting temperature so that it locally sinters and solidifies. After a cross-section is solidified, the platform moves down and another layer of powder is swept on top and so on until a 3D solid part is formed in the middle of the powder container.[2] Stereolithography, the motivating process for this thesis, uses liquid, photosensitive thermosets, like epoxy, that can be solidified by a UV laser. As the laser spot moves on top of a layer of liquid epoxy, the epoxy solidifies via a photochemical reaction. After forming a solid cross-section, the platform moves down and another liquid layer of epoxy is swept on top of the previous one and so on until a 3D solid part is formed within the liquid.[2]

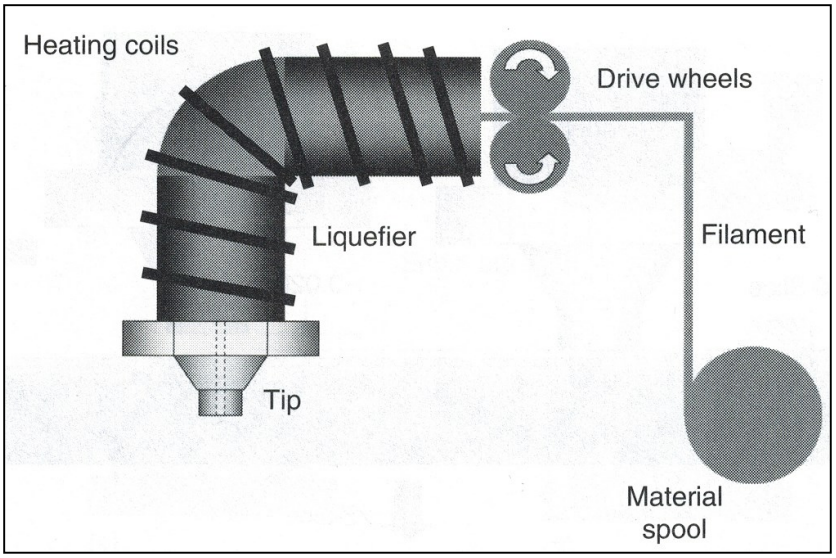


*Figure 1-2:* ***The fusion deposition modeling (FDM) process.*** *A thermoplastic filament is extruded through a hot end so that molten plastic is deposited on a platform to form layers.*[2]

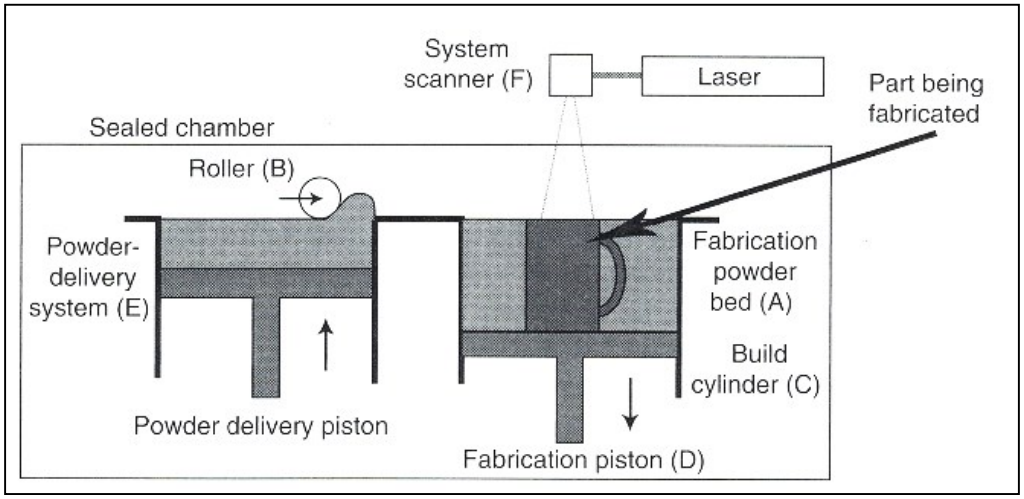


*Figure 1-3:* ***The selective laser sintering (SLS) process.*** *A chamber is heated up to below the melting point of the powder used and a powerful laser locally heats up a spot of powder above its melting temperature so that it sinters and cross-sections are formed.*[2]

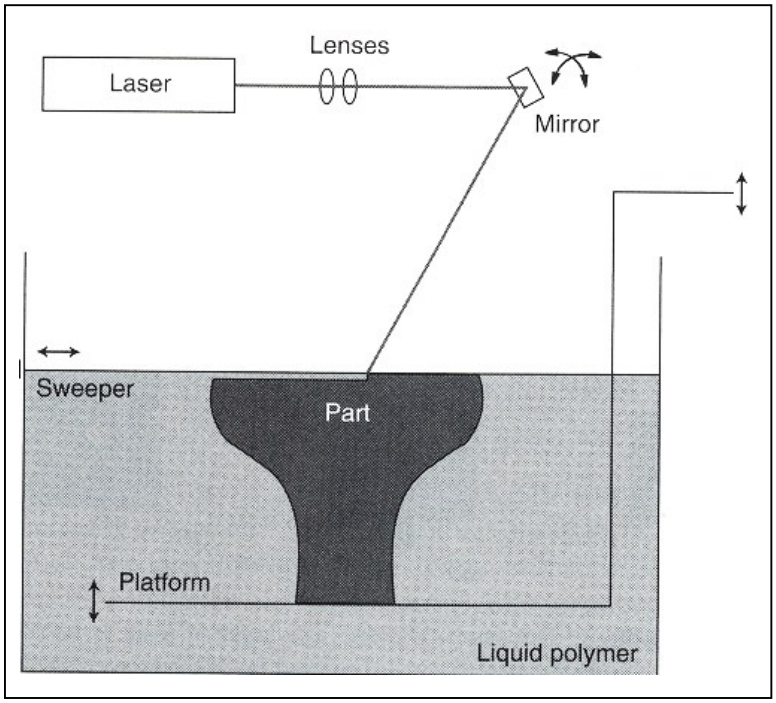


*Figure 1-4:* ***A stereolithography apparatus (SLA).*** *A photosensitive liquid material is used. A cross-section solidifies as laser traces in the XY plane. As solid cross-sections are built one on top of the other, a solid 3D part is formed within the liquid container.*[2]

The process of 3D printing has many advantages over formative and subtractive manufacturing processes, because of its additive nature. It eliminates the need for tooling and multiple machines, like lathes and mills, to do different manufacturing steps, like turning and milling, to make a given part and requires only a single 3D printer.[2] Using 3D printing, we can make impossible, or very difficult, to machine shapes[2,3] (Figure 1.5). In conventional manufacturing, one has to plan how the cutting edge will access the area where material needs to be removed. In 3D printing, there is no cutting edge to worry about allowing complex designs.

*Figure 1-5:* ***An example of a very complex 3D printed structure*** *that would be very expensive (if not impossible) to make using conventional machining.*[3]

Complete assemblies with movable parts can be printed in one shot given the right tolerances in the digital file[3] (Figure 1.6). Conventionally, different parts are machined separately, and then fastened and assembled in subsequent steps.

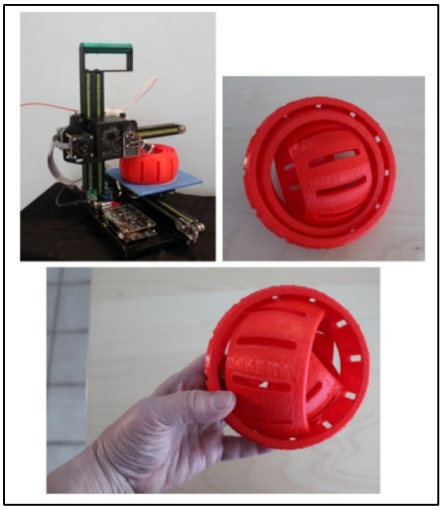

*Figure 1-6:* ***An example of an assembly with moving parts*** *printed all in one shot.*[3]

Furthermore, a 3D printer can print a given part with different materials, with different properties, in one shot[3] (Figure 1.7). Last, this additive approach results in very little or no material waste[2] as opposed to conventional machining which is, by definition, wasting material, by cutting the undesired sections of a block of material, to reach the desired shape. The most attractive feature of 3D printing is not just the time savings of the first advantage but rather the intricacies unlocked

by the later advantages[4] that relieve the designer of many manufacturing limitations. Despite all these advantages, 3D printing is mainly used for modeling and rarely for manufacturing because of material limitations[2].

*Figure 1-7:* ***An example of a part made of two different materials*** *(the orange, rigid, and the purple, flexible) printed at one shot.*[3]

The transformation of the 3D printing technology from rapid prototyping to rapid manufacturing is slowly becoming reality in a few industries and is expanding the limits of imagination of revolutionary applications. Such transformation is catalyzed by material developments. Murphy and Atalla[5] outlined how the main challenge of 3D printing for biomedical applications is material development. Bioprinting, another type of 3D printing using biocompatible materials or living cells, is an emerging and a rapidly expanding field. When proper materials have been developed, 3D printing is consistently used to produce customized prosthetics, surgical tools[5] and implants[6]. Furthermore, combined with stem cell research and tissue engineering, 3D printing is opening promising new frontiers in medical technology. Current research is aimed at developing a process whereby 3D designs are development using medical imaging, CT and MRI, to provide data. Then, printers 3D print scaffolds using biocompatible materials that provide the environment in which stem cells can grow to specialized cells and produce a transplantable organ[5]. These processes among others are outlined in Figure 1.8.

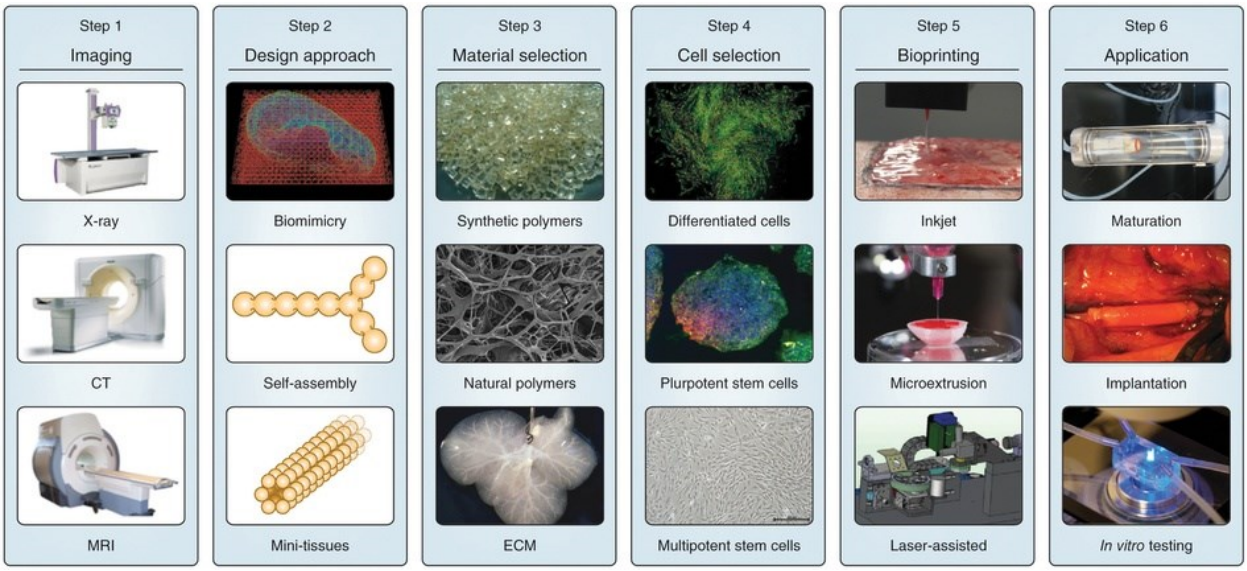


*Figure 1-8:* ***A summary of processes in biomedical research and applications where 3D bioprinting (step 5) is integral.***[5]

Once the capabilities have been developed to allow for 3D printing using metals in the SLS process, metal 3D printing started to creep into many high-stress applications, such as in the aerospace industry, to make functional parts. It, relatively cheaply, makes complex designs that are lighter, more efficient and with a lower "buy to fly" ratio.[6,7] "Additive manufacturing is a technology that I believe will fundamentally change the way we think about how we design our parts, how we manufacture components and ultimately how our products look and function," said Morris, GE Aviation's General Manager for Additive Technologies.[7] GE will be using metal 3D printing to make functional fuel nozzles for its LEAP jet engine that is on Boeing and Airbus aircrafts as of the end of 2015.[7]

NASA has already sent a 3D printer to the International Space Station to be used to produce spare parts on-demand and on-board reducing the need for frequent supply missions and mitigating the risk of unexpected failures.[8] This step marks only the beginning of the 3D printing era in space applications. Current materials research[9] shows that it is possible to 3D print using lunar dust positioning 3D printing to be a critical technology for future space exploration. This essentially implies that, in theory, all it would take to manufacture parts for a lunar base is sending a 3D printer that would use material found on the surface of the moon to build the base. 3D printing is

without a doubt the future of manufacturing and the highest barrier to entry for 3D printing to manufacture functional parts in any industry is material development.[2]

Even though metal 3D printing addresses some challenges for the technology to be used to make functional parts for the aerospace and automotive industries, it does not allow realizing its full potential. Many of those industries are already moving away from metallic parts to composites due to weight advantages and environmental benefits.[10] Metal 3D printing is energy intensive when compared to other 3D printing processes, like stereolithography, because of the thermal energy used to reach the high temperatures required.[2] Qualities like surface finish in printed parts also have to be improved due to the inherent porosity of the parts produced.[2] We believe that stereolithography 3D printing addresses many of those challenges and that it can provide the full potential of 3D printing in those industries.

Stereolithography 3D printing uses polymeric materials, like epoxy, to print so it is possible to 3D print using composites.[11] It is based on a photochemical reaction and does not require heat. Therefore, it is more favorable than SLS in terms of energy requirements.[2] It also offers a superior surface finish compared to SLS.[2] However, it has challenges of its own.

One such challenge is photo instability of the finished part.[2,12] To gain perspective on the problem, I visited Axis prototypes facilities, a company with more than 15 years of experience in providing 3D printing related services. During that visit, I learned that a critical issue is the photo instability of the cured material and that UV coating is often used as a short term fix. As an example of this, Mr Robin Clifford, Axis' managing director, talked about a project called the "bug eye" intended to show children what a bug's eye looks like. Stereolithography was used to make the part from an epoxy-based photocurable material (DSM Somos 11122). Initially, a clear UV coating was used to address photo instability issues. After approximately two to three months, the part cracked due to brittleness caused by photo degradation. A superior coating was later used to improve life time. Clearly, coatings only delay the problem as opposed to addressing the root cause of the photo instability. The next section discusses the chemical the root cause of the material photo instability.

## Chemistry

Photocuring is a crosslinking reaction (Figure 1.9) triggered by light. It has two modes: imaging and non-imaging. The imaging mode produces patterns while "overall" radiation is used in the non-imaging mode. Various detectable changes could occur in solubility, adhesion, color, phase (e.g. liquid to solid), refractive index and electrical conductivity upon radiation[13].

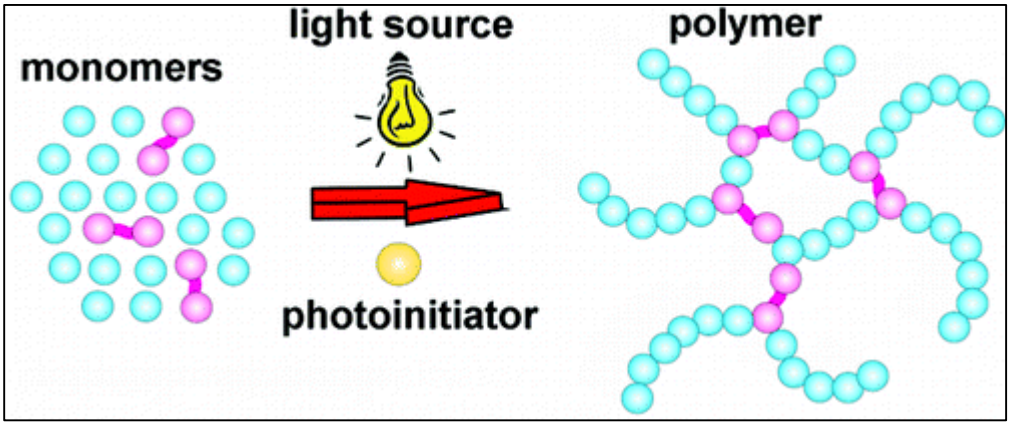


*Figure 1-9:* ***A schematic of the process of photocuring****. A photo initiator is excited by light of the proper wavelength and it initiates a photochemical reaction by which liquid monomers crosslink to solid polymer networks.*[13]

The first synthetic photopolymer, polyvinyl cinnamate, was developed in Kodac as a photoresist in printing plates.[13,14] In that application, metal plates are coated with polymers, exposed to sunlight (imaging mode) and washed with solvent (solubility change) to create an image. A vast array of high-impact applications followed since such as the manufacturing of printed circuit boards (PCB), and photocurable coatings, pigmented and clear, decorative and protective, of high-tech applications like biosensors, electrodes and optical fibers, and low-tech applications like furniture and floor finishes.[13,15]

The photocuring process is preferred to heat curing because of its inherent rapid crosslinking upon irradiation, lack of solvents and lower energy requirements.[13,16] For example, printing inks use photocurable polymers because of their rapid cure and reduced solvent emissions. Not only are photopolymers used in applications where heat is undesired like dental fillings but they are also favored for coatings as they replace expensive and energy-intensive ovens.[13,16]

Two distinct photocuring mechanisms exist: free radical and cationic.[17] Free radical polymerization is a mechanism that involves the formation of a free radical upon absorption of a light of a wavelength specific to the initiator. That radical activates the polymerization of acrylics via their double bonds. Two classes of free radical photo initiators exist: cleavage initiators and H-abstraction ones. Benzoin, an example of the first class, undergoes α-cleavage (Figure 1.10) producing radicals that initiate curing. This class of initiators has a high quantum efficiency and produces radicals with high reactivity but suffers from thermal instability and can only be stored at room temperature for limited time.[17]

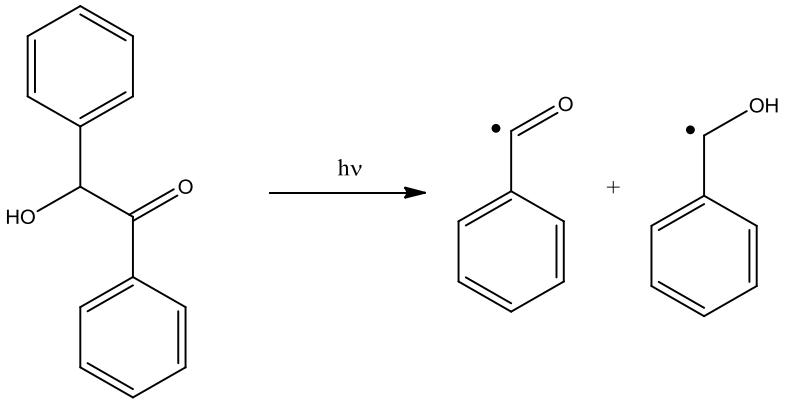


*Figure 1-10:* ***The α-cleavage free radical mechanism of benzoin initiated by light.***[17]

Benzophenone, an example of the second class, goes through a bimolecular reaction. Upon activation of benzophenone by light, a triplet is formed, which reacts with a hydrogen donor and, eventually, leads to the formation of two radical species (Figure 1.11). It is slower than that initiated in the first class. Radicals in both cases are vulnerable to quenching, particularly, by oxygen.[17]

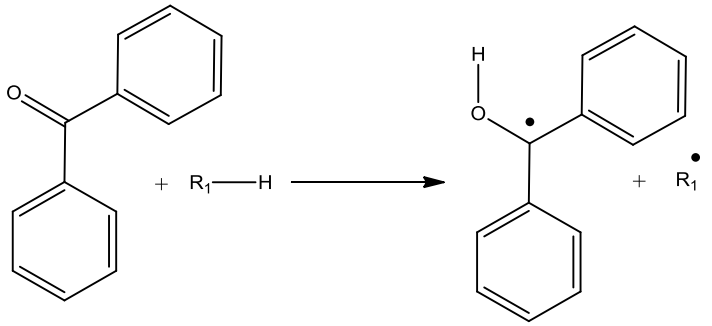


*Figure 1-11:* ***The H-abstraction free radical mechanism of benzophenone initiated by light.***[17]

Epoxy photocures cationically where an initiator decomposes upon activation by light to cations and, eventually, produces a protonic acid triggering the cationic polymerization of epoxy monomers (Figure 1.12).[16,17,18]

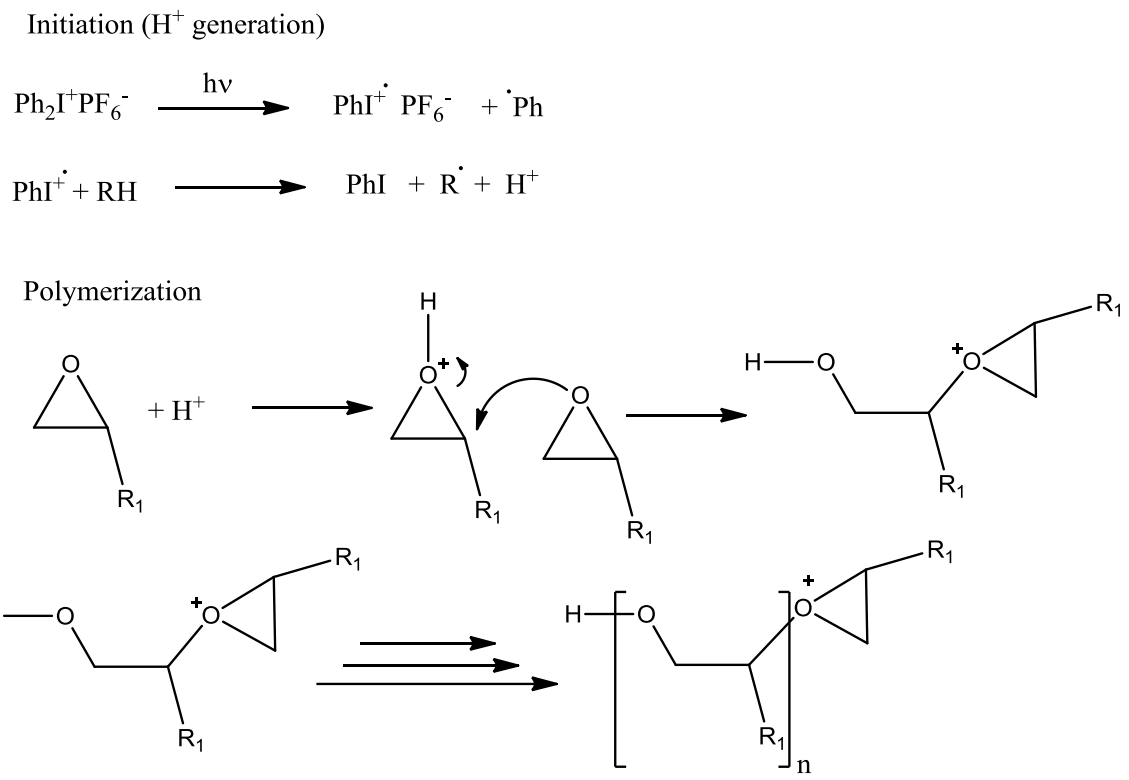


*Figure 1-12:* ***A general schematic of the cationic photocuring mechanism.*** *Upon irradiation, cationic molecules decompose to cations that oxidize materials and produce protons leading to the crosslinking of epoxy.*[17,18]

The first such initiator is aryldiazonium salt[16] developed at Can Company[19] that produces Lewis acid to photocure epoxy. It photocures epoxy rapidly without oxygen inhibition and has minimal sensitivity to water. More relevantly, unlike free radical polymerization, it can cure epoxy. However, it suffers from poor latency due to thermal instability as it spontaneously gels within hours without radiation. Later on, Crivello[16] developed the more stable diaryliodonium salts as well as an array of other onium salts. A prerequisite for those salts to photoinitiate epoxy curing is that the anion must be non-nucleophilic so that the cationic species is not quenched by them and remains available to catalyze the production of protons. In fact, anions determine initiation

efficiency and acid strength. On the other hand, the cation is the component that absorbs the light and, consequently, determines the photochemistry of these compounds and controls the absorption wavelength, quantum yield and thermal stability.[16]

Many of the preferred resins used in stereolithography 3D printing are epoxy-based curing via a cationic photoreaction in an imaging mode leading to phase changes, from liquid to solid. UVA lasers (around 365nm) are used to locally photocure the resin into the desired three dimensional shapes. The resin contains UVA-sensitive cationic initiators.[13,16,17] The solar spectrum on Earth starts at about 300nm and everything below is blocked by the ozone layer.[12] This means that solar light on Earth also includes UVA. That UVA excites the catalysts in the 3D printed material even after printing leading to undesired reactions and continuous changes in properties causing part failure, as shown by the schematic in Figure 1.13.

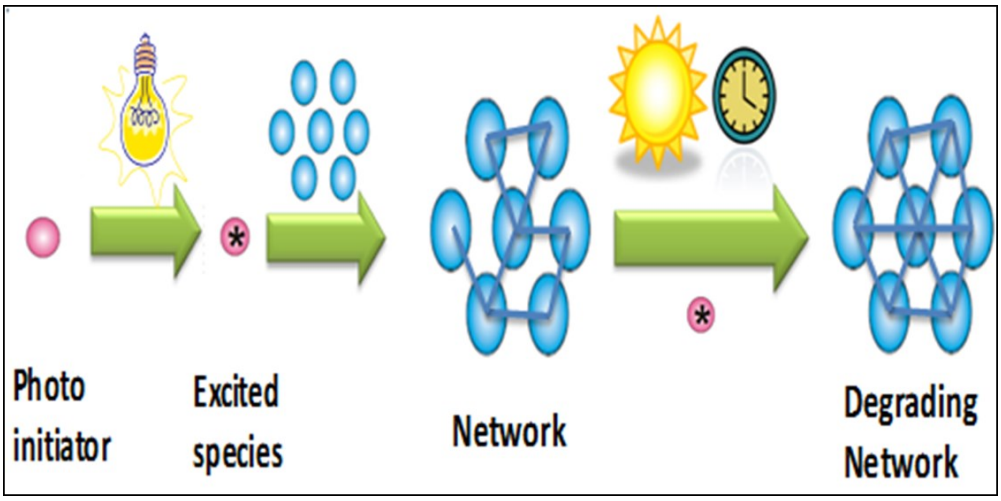


*Figure 1-13:* ***A schematic of the photocuring process and photoinstability of cured materials.*** *The same UVA in the light source triggering the curing reaction also exists in the solar spectrum on earth triggering undesired reactions that lead to eventual part failure.*

The same problem also exists in coatings, particularly the ones where monomers can be readily cured by UVA light without the need of additives. Hare[12] explains that reactive species are produced by absorbing light from 300-380 nm in the atmosphere leading to further curing causing embrittlement or undesired changes in properties. Even in polymers that do not readily absorb UVA, additives can lead to the same problem. Hare further explains that this is mitigated by adding

pigments that absorb or reflect UVA or luminescent pigments that re-emit the energy in higher wavelength rays. These mitigations only slow down the process.

To address the root cause, we propose that initiators sensitive to light only below 300 nm be used to initiate the photocuring of epoxy resins. This is the central idea around which the activities of this research revolve. Addition of various chromophores during the synthesis of those onium salts allow for the manipulation of their absorption wavelengths.[16] According to Xiao et al[20], metal complexes have good absorption in the visible region, long life time and proper redox potentials required to produce reactive species, but they are costly. The use of dyes as photosensitizers broadens the range of absorption wavelength. They have relatively lower cost and toxicity but are still sensitive to only some wavelength(s). The objective of all reviewed research is to develop initiators with discrete band gaps in the visible region. Synthesizing for bandgaps in the NIR is the following milestone. The goal of this thesis is to develop initiators responding only to light below 300 nm (the opposite direction).

Another class of initiators is semiconducting material to photocure polymers based on electrochemical principles.[21] Kamat[22] demonstrates that a photocured film of 1-vinylpyrene can be formed on a n-GaAs electrode in an electrochemical cell upon irradiation by visible light (>460 nm) or electrochemically on a $SnO_2$ electrode by the application of an anodic potential. An aqueous dispersion of ZnO powder can photopolymerize methyl methactylate.[23] The rate of photocuring using ZnO accelerates by using ZnO "quantum dots" according to Hoffman et al.[24] Similarly, butylmethacrylate is showed to photopolymerize by ZnO quantum dots and other semiconducting nanoparticles like CdS.[25] Hoffman et al[24] attribute the acceleration to the increase in surface area of the semiconducting nanoparticles. No polymerization is observed when bulk-sized ZnO is used in either studies conducted by Hoffman et al[24] or the ones conducted by Stroyuk et al[25]. All mentioned reactions are in the free radical category. When the semiconductor absorbs light of an energy that corresponds to the semiconductor's band gap, an electron-hole pair is created. The interaction of that pair with polymeric materials and solvents, depending on the specific reaction, eventually leads to the creation of radicals that polymerize materials containing double bonds allowing them to corsslink. However, Hoffman et al[25] also found that below a certain size, the reaction rate decreases with the size of the particles used. They attribute that to the increase in electron-hole recombination rate and an increase in surface defects. Another hypothesis could be

that the absorption wavelength of the quantum dots is blue shifted away from the peak wavelength emitted by UV lamps as the quantum dots' size decreases reducing the number of electron-hole pairs created to initiate the reaction.

This quantized effect constitutes an interesting research opportunity as it implies that quantum dots can be "tuned". That is to say that the range of wavelength they are sensitive to can be engineered as needed by many applications as demonstrated earlier. The challenge is that semiconducting nanoparticles have never been shown to photocure epoxy or catalyze cationic photocuring before. To tackle such a problem, the physics involved in quantum dots is outlined.

## Physics

Quantum dots are nanoparticles that are smaller than a critical size and exhibit the quantized effect. The quantized effect implies that below a critical size, the band gap energy of the semiconductor becomes a function of its size. The band gap energy of the quantum dot increases as its size decreases. This is referred to as a blue shift as the increase in band gap is a decrease in absorption wavelength so colored materials shift to the blue end of the visible spectrum (Figure 1.14). Some semiconductors, like ZnO and $TiO_2$, absorb in the UV region.[26,27]

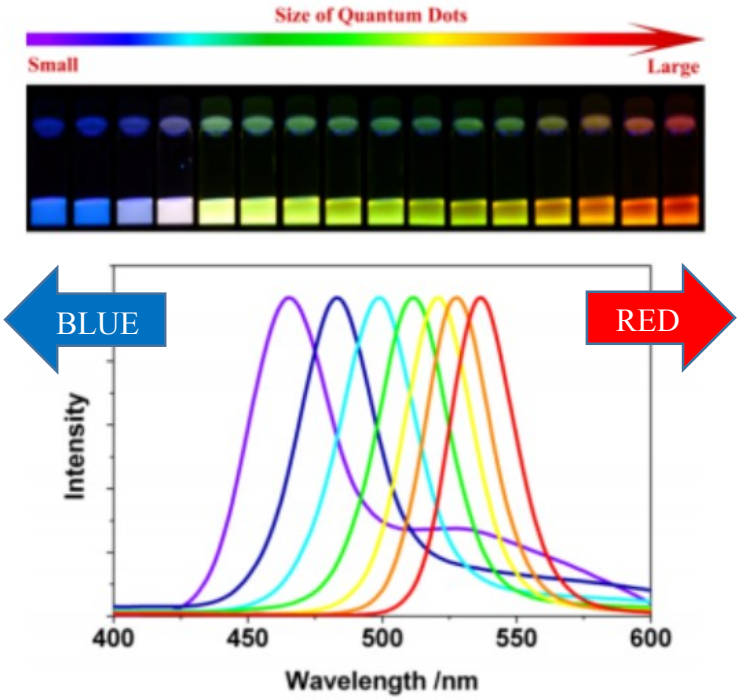


*Figure 1-14:* ***The quantized effect of tunable emissions****. CdSe Quantum dots of different sizes excited by UVA light.*[27]

The band gap energy of a semiconductor is the energy required to create an exciton, an electron-hole pair. The electron and the hole in the exciton are attached to each other via electrostatic forces that is a function of the distance between them within the lattice. In bulk size, the size of the exciton, otherwise known as the Bohr radius, is a material property and so is the band gap energy required to overcome the electrostatic forces. In crystals smaller than the Bohr radius of the material, the lattice is simply too small to allow enough distance between the electron

and the hole to overcome those electrostatic forces using only the band gap energy of the bulk material and, therefore, the exciton would require more energy to sustain itself at that smaller separation, increasing the effective band gap energy of the quantum dot.[28,29]

In the bulk regime, a free electron model can be used, though it is an over simplification. In that model, the crystal is considered infinite with disregarded outer boundary conditions. Therefore, the wave function is periodic and a wave vector k is used.[29] Finally, the energy states are estimated by Equation 1-1:

$$\mathrm{E}_k = \frac{\hbar^2 k^2}{2m_h} \qquad (1\text{-}1)$$

Here, $\hbar$ is reduced Plank's constant and m is the mass of the particle.

FIGURE 1.15 shows the energy states in k space in a direct semiconductor of its valence and conduction bands. The difference between the maxima of the valence band and the minima of the conduction band constitutes the band gap energy of the bulk material.

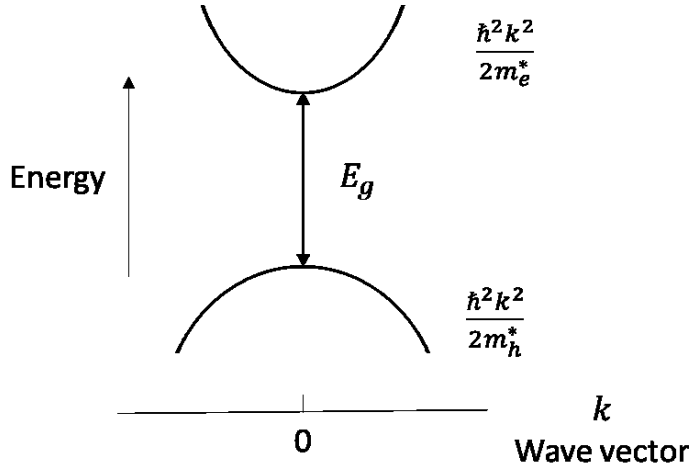


*Figure 1-15:* ***Single particle energy states*** *as a function of wave vector k in a direct band gap semiconductor.*[28]

In the quantized regime, the electron is "confined", and the crystal can no longer be considered to be infinite. Consequently, the shift in energy (the increase in band gap energy) can be estimated using the "particle in a box" model. In that regime, the energies are discrete and quantized.[27] The energy of each state is estimated by Equation 1-2:

$$E_n = \frac{\hbar^2 \pi^2 n^2}{2m^* R^2} \quad (1\text{-}2)$$

Here, $m^*$ is the effective particle mass.

The final band gap energy of a quantum dots is higher than the band gap energy of the bulk material by the quantized energy of the edge states (n=1) of the exciton (electron and hole) as shown in Equation 1-3.

$$E_g^{QD} = E_g^{bulk} + \frac{\hbar^2 \pi^2}{R^2} \left(\frac{1}{m^*_e} + \frac{1}{m^*_h}\right) \quad (1\text{-}3)$$

Here, $m^*_e$ and $m^*_h$ are the effective masses of the electron and hole, respectively.

This equation clearly demonstrates that the increase of the band gap energy of the quantum dot over that of the bulk material is a function of its size. The smaller the quantum dot, the bigger its bandgap energy, the smaller its absorbance wavelength (blue shift). Another conclusion is that, the energy states are discrete and quantized as a function of n. This contrasts the states in bulk size where R is so big that the whole term is negligible. In reality, the states are still discrete in bulk size but the differences between states are so small that the density of state appear as a continuous function of energy. Note that at bulk size, the second term in Equation 1-3 will simply disappear and go back to Equation 1-2. Note that all the physics presented here is over-simplified and in no way intended to be comprehensive or adequately model the system involved in this research.

The unique properties of quantum dots, particularly having tunable absorbance and emission peaks, make them advantageous for many applications: optics, medical imaging and catalysis.[26,27] They are used in light emitting diodes (LEDs) to replace their organic counter parts because of their narrow emission peaks (necessary for high quality images), they are more thermally stable, and their colors do not change over time (red, green and blue pixels can be made of the same material so they do not have different life times as they do in organic compositions).[27]

Exciting research is underway so that quantum dots replace organic agents in medical imaging (radioscopic or magnetic). Quantum dots are more stable than their organic counter parts, less vulnerable to photobleaching, and have higher quantum yields. The tunability of their absorbance and emission peaks as well as the broadness of their absorbance peak and narrowness of their emission peaks allow for high resolution multicolor imaging using a single light source,

avoid autofluorescence noise and minimize crosstalk between different dyes whose emissions overlap. Quantum dots can have shells to reduce toxicity, and increase their biocompatibility and circulation time.[27,30] They can also have bio-active targeting ligands to increase their specificity. An example is in-vivo cancer targeting dots developed for imaging and therapeutic purposes.[31]

Furthermore, quantum dots are showing a lot of promise in catalysis and photovoltaics. An example is the already mentioned photocuring of acrylics.[24,25] In solar cells, the path started from using semiconducting plates to split water using solar light for the first time.[32] Recently, semiconducting PbS coated ZnO quantum dots has been demonstrated to have the highest certified efficiency of 8.55%.[33] Such efficiency is achieved by band energy engineering where the energy levels are tuned in such a way where the excited electron is essentially blocked from recombining with the hole. Many of those processes, whether in splitting water or the photocuring of acrylics, involve the existence of intermediary protons. As mentioned before, protons have the ability to open up the epoxide rings so that they crosslink.[17,18] We hypothesize, as outlined and studied in the following chapter, that in the presence of epoxy, those intermediary protons, catalyzed by a semiconductor after irradiation with light of energy corresponding to its bandgap, would open up the epoxide rings and cure the epoxy.

# 2. Photocuring epoxy with quantum dots for 3D printing.


## Abstract

Photocuring of polymers is fundamental to many applications: dentistry[13,16], coating[13,15] and stereolithography 3D printing[13,16,17]. One challenge is the wavelength of the light used to initiate photocuring.[12] In coating applications, it is often desirable to photocure with solar light to eliminate the cost of a UV lamp.[20] In stereolithography 3D printing, which motivates this work, it is desirable to photocure only with light outside of the solar spectrum on Earth to produce parts that are photostable in the end use. Tunable initiators are therefore needed.

Semiconducting nanoparticles have previously been shown to photocure acrylic resins via a reduction reaction.[24,25] However, epoxy photocures via a cationic process typically using a cationic initiator.[16,17] Here, we use semiconducting nanoparticles instead of a cationic initiator in the photocuring of epoxy for the first time. If small enough, semiconducting nanoparticles are quantum dots with tunable absorbance.[26,27] In this work, bulk and quantized $TiO_2$ nanoparticles are used to initiate the photocuring process of epoxy resin and a reaction mechanism is presented. We study the effects of process variables (alcohol type and concentration, nano particle crystal structure, surface area and concentration and the presence of an electron scavenger) on the kinetics of the reaction.


## Introduction

Photocuring of polymers is integral in many applications that require different specifications with respect to the curing behavior. For example, stereolithography 3D printing requires a fast reaction that produces products that are stable in the end-use.[13,16,17] Existing photo initiators typically respond to UVA (365 nm) which is within the solar spectrum on Earth.[12,16,17] Products containing such initiators continue to react during its use rendering printed parts unstable with changing, even deteriorating, properties.[12] Photoinitiators that respond to different wavelengths, ie. with tunable bandgaps, are therefore desirable. Our approach is to identify a chemical process in which semiconducting nanoparticles initiate epoxy photocuring. Their band gap can be tuned via the quantized effect[26,27] by selecting their size to absorb only outside the solar spectrum (above 4.1 eV or a wavelength below 300 nm) allowing for photostable materials in the end-use.

There are two photocuring mechanisms: free radical and cationic polymerization.[17] Quantum dots have previously been shown to initiate the free radical photocuring reaction of acrylics.[24,25] A similar concept[21] will be used here to oxidize an alcohol to produce protons required for the cationic photocuring of epoxy.

In the typical cationic photo polymerization, cationic initiators absorb light of the appropriate energy, they produce cations that oxidize an alcohol releasing protons. The protons open epoxide rings and allow crosslinks to form. Producing sufficient protons on demand is the requisite to photocuring epoxy.[16,17,18]

There is extensive literature on the development of initiators with specific light absorbances suitable to different applications. Crivello developed the first onium salt initiators to replace thermally cured enamel in electrical applications with a photocured polymer saving energy.[16] This triggered much of the research on cationic polymerization and many applications like coating[13,15] and 3D printing[13,16,17]. As discussed by Xiao et al (2015)[20], metal complex initiators absorb light in the visible region, and have a long lifetime and the proper redox potentials required to produce the reactive species, but they are costly. Dyes, in comparison have a lower cost and toxicity but are still sensitive to the wavelength(s) of the light source. The work reviewed by Xiao et al involves initiators with discrete band gaps in the visible region. Xiao states that the next challenge is to synthesize initiators in NIR. Our goal is to identify an initiator for photocuring epoxy that is responsive only to radiation of wavelength less than 300 nm.

The principles of oxidation and reduction[11] via semiconducting nanoparticles were implemented when Fujishima and Honda first demonstrated the splitting of water with solar light using a semiconducting plate[13]. The water is oxidized by the photogenerated holes, to generate $O_2$ and the protons are reduced by the photogenerated electrons to form $H_2$ gas. As most semiconductors, and most notably $TiO_2$, do not promote the reduction of protons by themselves, water splitting can only occur if the semiconductor is electrically connected to a metal electrode, most often platinum. Indeed, reduction of protons (water) readily occurs at such electrode. The realization that semiconducting nanoparticles can promote redox reactions has generated a flurry of activity in the domain of photocatalytic depollution, whereby an organic pollutant is decomposed by a series of oxidation (and reduction) processes. Thus semiconductors can catalyze the photodecomposition of alcohols.[8] In this case, it is generally admitted that the first step is the

oxidation of the alcohol by a photogenerated hole, to yield a ketone and a proton. Our hypothesis is that, in the presence of epoxy, these protons would open epoxide rings and initiate a curing reaction.

Figure 2.1 shows the proposed mechanism for the photocuring of epoxy. The excitation of the semiconductor produces an exciton: a hole and electron pair. The hole oxidizes the alcohol producing a ketone and a proton. The protons then open the epoxide rings to crosslink and photocure. Here, we verify the ability of semiconducting nanoparticles to photocure epoxy and investigate the validity and the implications of the proposed mechanism.

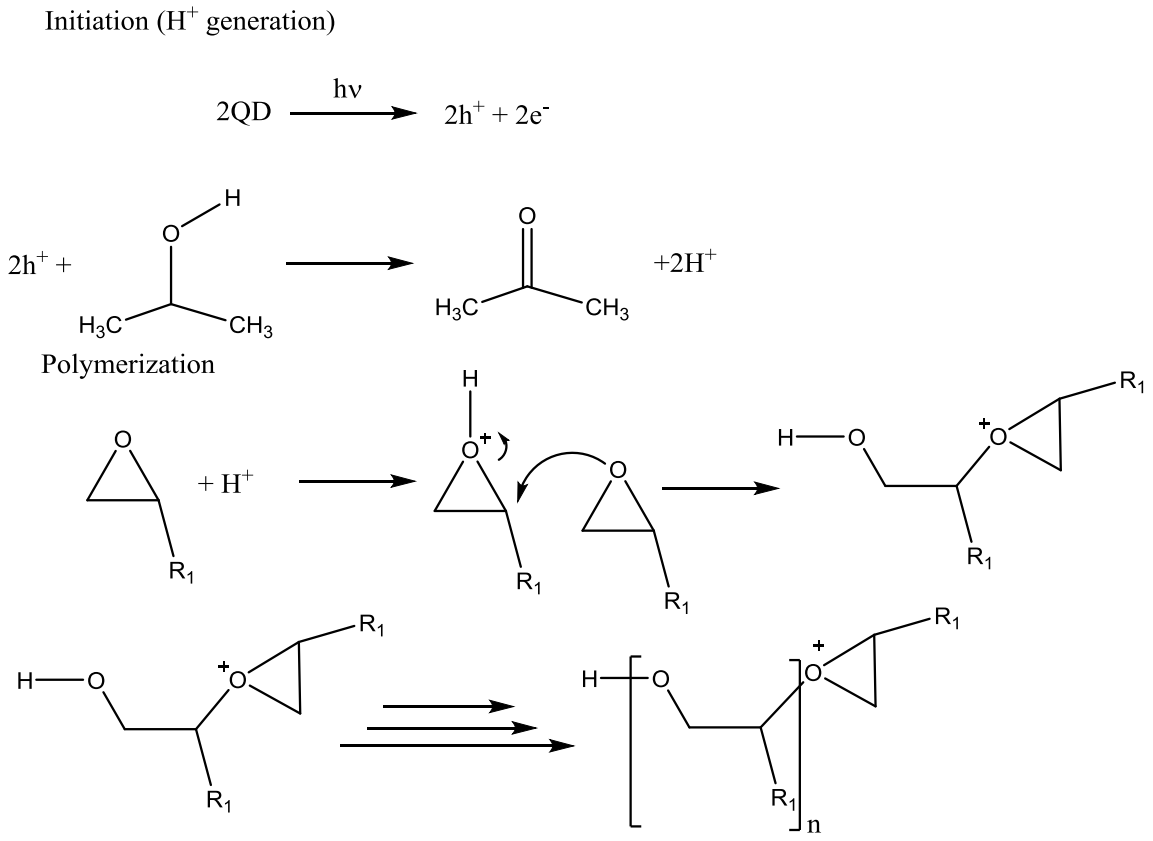


*Figure 2-1:* ***Proposed mechanism of the photocuring of epoxy using semiconducting nanoparticles.*** *After excitation, the hole ($h^+$) oxidizes the alcohol to produce protons that activate epoxide groups to crosslink.*

## Materials and methods

Epoxy, 1-4 cyclohexane dimethanol diglycidyl ether mixture of cis and trans (technical grade), isopropanol (99.5%), 2-phenethyl alcohol (99%), 1-phenethyl alcohol (98%), Methyl

Viologen dichloride hydrate (MV) (98%), hydrogen bromide solution in acetic acid (33 wt%), crystal violet indicator, bis (4-methylphenyl) iodonium hexafluorophosphate (98%), P25 and bulk anatase titania (25 nm size, 50 $m^2/g$ surface area, 99.7% purity; peak absorbance of bulk anatase is at 260 nm) from Sigma Aldrich and anatase titania 5 nm (356 $m^2/g$, 99.9% purity, peak absorbance at 248 nm) and 10 nm (255 $m^2/g$, 99%, peak absorbance at 260 nm) from mkNANO were used as received. Figure 2.2 shows the chemical structures of the alcohols used. P25 is one of the best known photo catalysts and a mixture of anatase (87%) and rutile (13%) with an average diameter of 25 nm and a surface area of 50 $m^2/g$ is used as purchased from Sigma Aldrich. The peak absorbance of all anatase nanoparticles is obtained from UV-VIS absorbance spectra (Appendix 1).

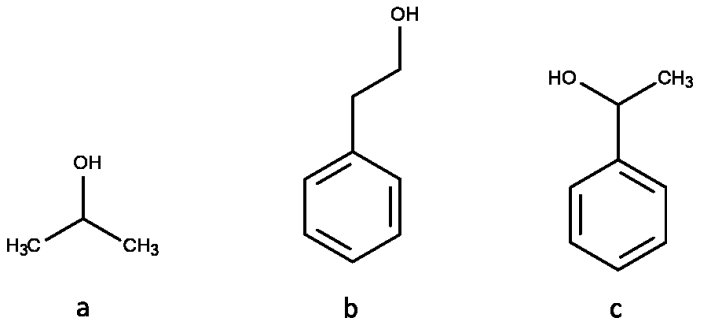


*Figure 2-2:* ***Chemical structure of the alcohols.*** *a) isopropanol, b) 2-phenethyl alcohol and c) 1-phenethyl alcohol. Note that the carbon carrying the alcohol group in 1-phenethyl alcohol is more substituted than that in 2-phenethyl alcohol.*

Mixtures (1.5 g) consisting of epoxy , alcohol (isopropanol, 1 or 2-phenethyl alcohol), MV and nanoparticles (P25 or anatase -25 nm, 10 nm or 5 nm) were stirred overnight and sonicated for 30 minutes (5 seconds on, 20 seconds off) using a Misonix, sonicator 3000, sonicating probe. In some control samples, MV and/or nanoparticles were excluded. The mixtures were blade coated on microscope slides to make films that were radiated in a photo chamber, UVP (CL-1000L), for up to 150 hours with a light intensity of 4 $mW/cm^2$ at the surface of the samples.

The percentage of cure were measured using Fourier transform infrared (FTIR) spectroscopy (NEXUS in ATR mode) with 64 scans at 1 $cm^{-1}$ resolution between 600 $cm^{-1}$ and 4000 $cm^{-1}$. Titration was performed according to ASTM-D1652-97. Prior to titrations, films were

dissolved in glacial acetic acid, stirred for more than 12 hours and then 2-3 drops of 0.1% solution crystal violet indicator in glacial acetic acid were added. The glass slide was weighed with and without the film to obtain the weight of the dissolved film. A solution of HBr and glacial acetic acid was used to titrate the solutions. The molarity of the HBr solution was standardized and measured using known quantities of potassium acid phthalate. During the titration, 0.5 mol/L of HBr solution was used for data points where less curing was expected and 0.06 mol/L for the later points where higher curing is expected. A highly diluted dispersion of nanoparticles in deionized water (<0.0001g/ml) is sonicated and used for UV-Vis scans from 300-800 nm (Cary 100 Bio UV-Vis spectrometer) with a sampling frequency of 1 nm.

## Results

### Verification of proposed reaction mechanism

In order to verify the proposed reaction mechanism we must prove that semiconductors initiate curing and that it is triggered by light.

To prove that semiconductors initiate curing, a system consisting of epoxy and alcohol only (control 1) is compared to a system consisting of epoxy, alcohol and semiconducting nanoparticles (sample) and a system containing epoxy, alcohol and a commercial photoinitiator. Their FTIR spectra after irradiation are shown in Figure 2.3 and are referenced to an initial spectrum (epoxy, alcohol and commercial initiator, no irradiation). Note that the initial spectra of the different mixtures are practically identical as shown in Appendix 1 and, consequently, only that of the mixture containing a commercial initiator is shown in Figure 2.3.

When using the commercial initiator system, the characteristic epoxide peak around 900 $cm^{-1}$ in FTIR disappears after illumination, which is indicative of the ring-opening of the epoxide, and therefore of the epoxy resin curing. During the curing, no other peak appears, which can be explained by the fact that during the polymerization no chemical bond is changed by the polymerization, except the strained CO bonds becoming unstrained CO bonds. The percentage of cure can be estimated by normalizing the area of the epoxide peak to that of the aliphatic peaks in the 3000 $cm^{-1}$ region as per Equation 1.

$$Percent\ of\ cure = \left(1 - \frac{A_{900}}{A_{3000}}\right) \times 100\% \quad (1)$$

Note that this system takes more than 40 minutes to fully cure, much longer than it does in stereolithography 3D printing where the illumination density at the level of the sample of the laser is orders of magnitude higher than the 4 $mW/cm^2$ due to the lamp used here.

The FTIR spectrum of control 1 (no nanoparticles) after 133h of radiation is unchanged as compared to the initial spectrum. However, the FTIR spectrum of the system containing the semiconducting nanoparticles shows two significant changes due to radiation: the epoxide peak at 900 $cm^{-1}$ disappears, as with the commercial initiator, and a new, large peak at 1700 $cm^{-1}$ appears. The peak at 1700 $cm^{-1}$ is characteristic of C=O related to acetone which is a side product of the proposed reaction mechanism when isopropanol is used. Therefore, the new peak is consistent with the proposed reaction. This peak is unique to the proposed reaction mechanism as it does not appear in the epoxy system containing commercial cationic initiator.

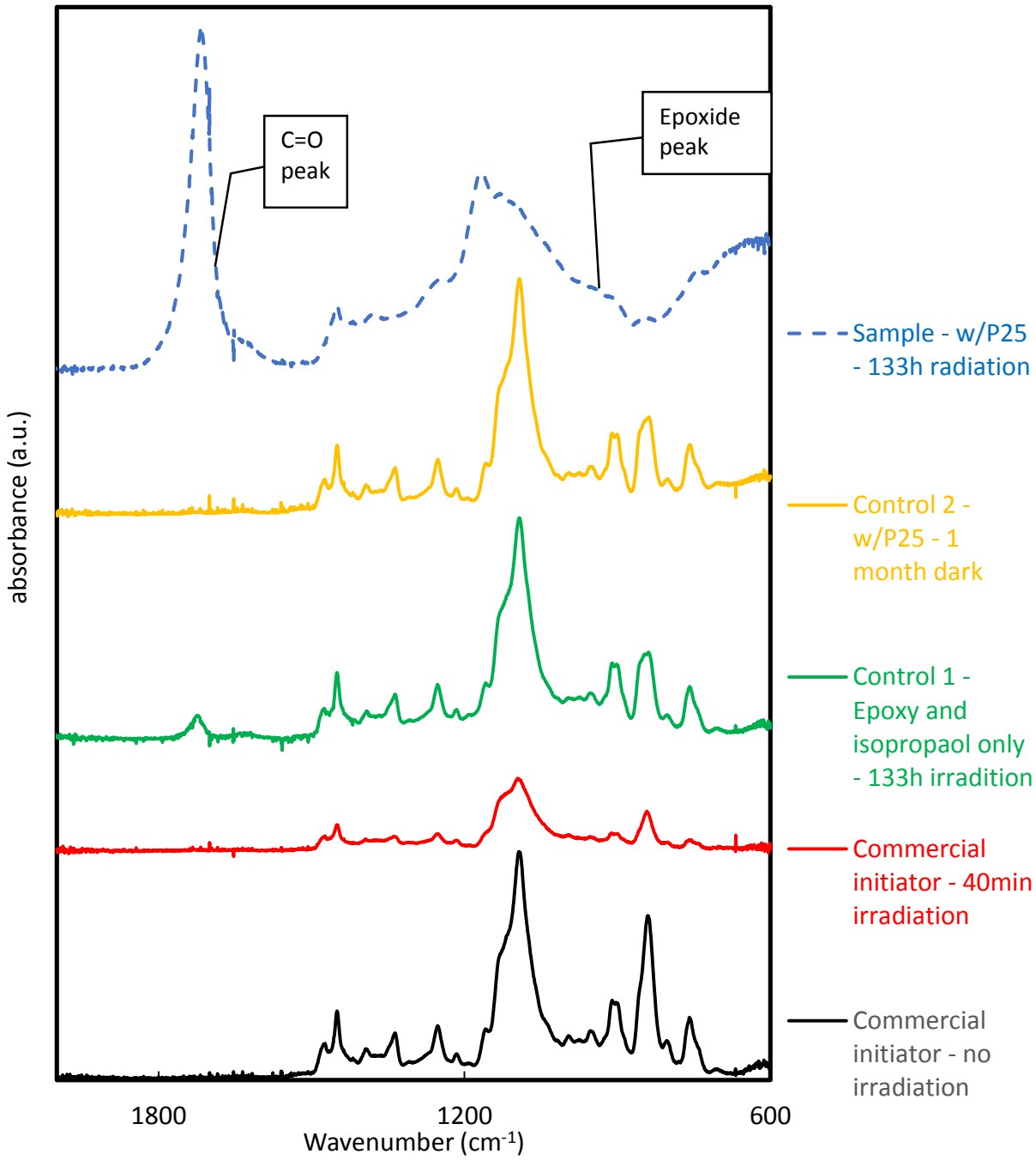


*Figure 2-3**: Effect of initiator and radiation exposure on FTIR spectra** of systems containing epoxy and isopropanol (5 wt%). The catalyst, either P25 or commercial initiator, (5 wt%) and radiation time are as specified.*

Figure 2.4 shows the percentage of cure observed in both the control and sample systems as a function of irradiation time. These results are calculated from FTIR data using Equation 1.

The shape and pattern of the curing curve is consistent with what one would expect from a typical epoxy and clearly, no reaction is occurring in the control system.

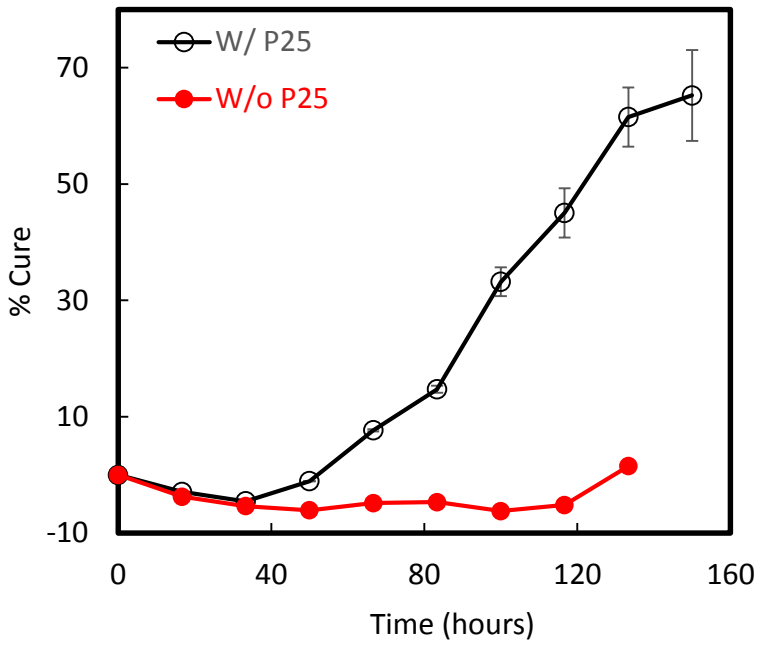


*Figure 2-4:* ***Curing Reaction verification.*** *Systems contain epoxy and isopropanol (5 wt%). One system includes 5 wt% of semiconducting nanoparticles (P25) while the control system does not.*

To confirm that the reaction is triggered by light, a system consisting of epoxy, alcohol and semiconducting nanoparticles (control 2) is prepared and kept in the dark for 30 days. The FTIR spectrum of control 2 does not change as compared to the initial spectrum (Figure 2.4) indicating that no reaction takes place.

To summarize, these results indicate that the presence of semiconducting nanoparticles under irradiation triggers a reaction that consumes epoxy and produces C=O containing side product(s) supporting the proposed epoxy curing reaction mechanism (Figure 2.1).

Verification of percentage of cure determined from FTIR spectra

The absorbance of the aliphatic peaks (3000 $cm^{-1}$), used in normalization (Equation 1) to determine percent of cure, decreases during curing. Unfortunately, the absorbance of all FTIR peaks changes while curing and in the absence of an appropriate internal standard, we must provide an independent verification of the results. Equation 2 shows that FTIR absorbance is a function of factors whose effects are minimized or eliminated by normalization.

$$A = \varepsilon bc \qquad (2)$$

Here, A is absorbance, $\varepsilon$ is molar absorptivity, b is path length, and c is molar concentration of the moiety. The decrease in the absorbance of the aliphatic peaks may be due a change in the effective path length which is eliminated with normalization, however, the possibility that it may be due to a reaction cannot be disregarded. As an independent verification of the FTIR results, the percentage of cure is determined through titration with HBr (Figure 2.5). The titration data confirms the previous results and FTIR can therefore be considered a reliable technique to monitor the epoxy curing reaction.

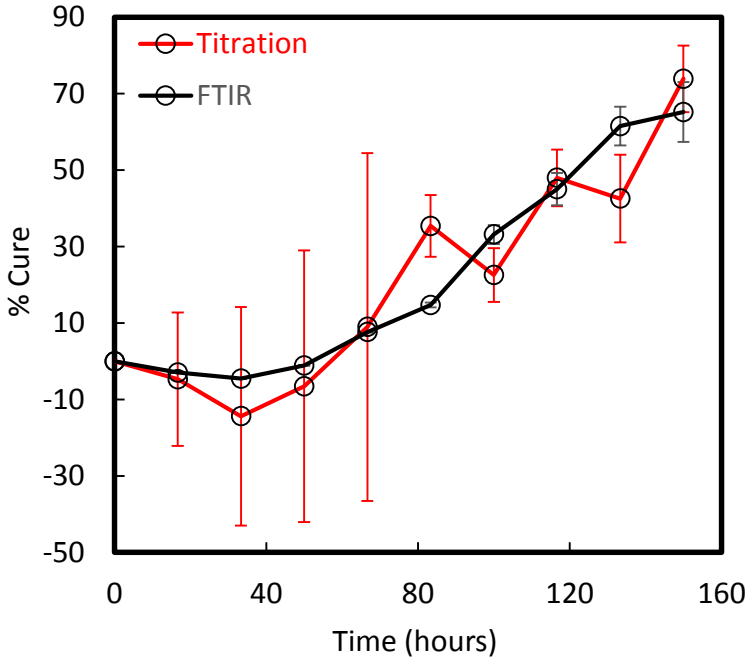


*Figure 2-5:* ***Validation of FTIR-based technique for determining % Cure.*** *Systems contain epoxy, isopropanol (5 wt%) and P25 (5 wt%). Titration performed with HBr. Note that the short time titration measurements have large error bars due to the high concentration of titrant.*

Limiting factors of the proposed reaction

The nanoparticle photocuring reaction is slower than that observed with the commercial initiator therefore we next address the factors that are limiting the rate of reaction: the fate of the excited electron and the stability of the radical intermediate in the alcohol oxidation.

The reaction mechanism as it stands is incomplete; the fate of the excited electron is undefined. The excited electron has many possible paths including recombining with the hole and reacting with the proton both of which have a negative effect on the desired reaction. If the electron recombines with the hole, the alcohol will not be oxidized and there will be no curing reaction. If the electron reacts with the proton to produce hydrogen, the proton will not be available to open the epoxide ring and initiate the curing reaction. However, this latter reaction is not very probable, as $TiO_2$ alone is not able to reduce protons. If adventitious oxygen is present in the system, the electron may reduce $O_2$ to form the superoxide anion $O_2^-$ as well as other highly reactive species. Here, an electron scavenger[34], methyl Viologen (MV), is used to consume the excited electrons.

To evaluate this approach, equivalent systems with and without MV are irradiated (Figure 2.6a). A control mixture (Appendix 1) without nanoparticles verifies that no reactions are caused by MV under irradiation. The induction time of the epoxy reaction is shorter in the sample with MV than that without MV supporting the importance of electron scavenging.

According to the proposed mechanism isopropanol oxidizes to acetone and produces two protons. The reaction of the alcohol with a hole entails the extraction of one hydrogen atom to form a proton, thus generating an intermediate radical. The ease with which the hydrogen atom is removed from the alcohol (and therefore the yield of the reaction) depends on the stability of the radical. The radical stability depends on the level of substitution of the carbon: the more substituted the carbon, the more stable the radical and the more likely it is for the alcohol to be oxidized. Furthermore, radicals adjacent to phenyl groups (so called benzyl radicals) are stabilized by resonance. In order to explore this effect, two isomeric alcohols are used: 1- and 2-phenethyl (structures are shown in Figure 2.2). With 1-phenetyl alcohol, the radical is stabilized by resonance and by the fact that it is a secondary alcohol. The results are in Figure 2.6b: the reaction exhibits a shorter induction time with the more substituted alcohol than with the less substituted alcohol. Controls, without nanoparticles, exhibit no curing (Appendix 1). These observations are consistent with the proposed mechanism.

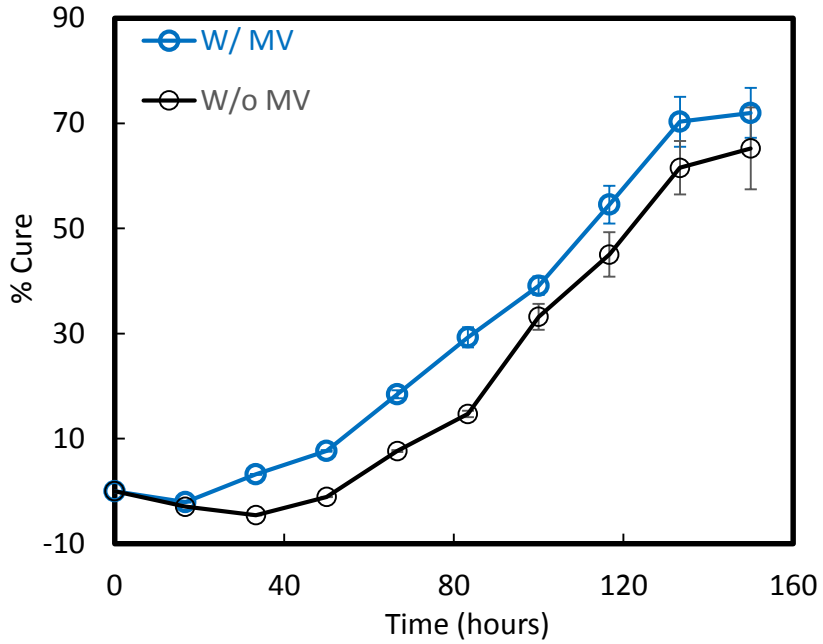


**(a)**

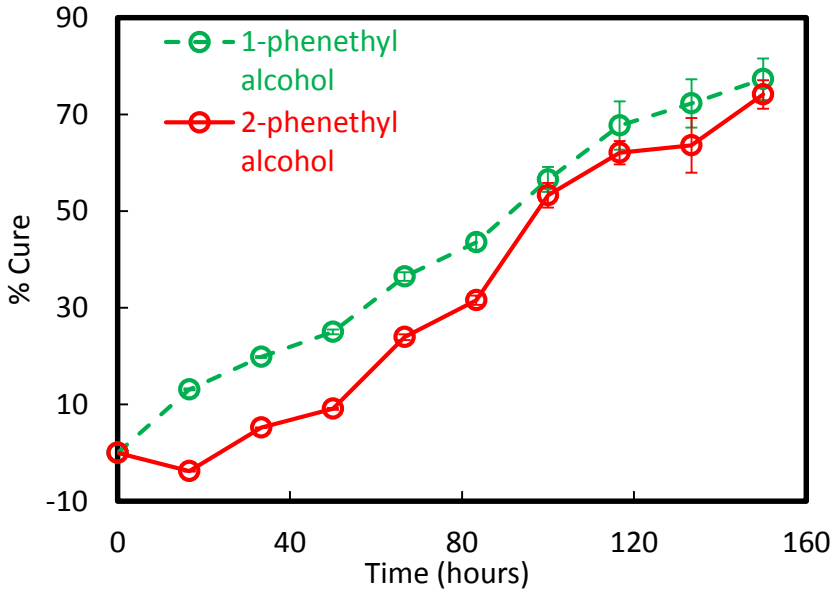


**(b)**

*Figure 2-6:* ***Limiting factors of proposed reaction mechanism.*** *Systems contain a) epoxy, isopropanol (5 wt%), and P25 (5 wt%) with and without MV (0.5 wt%), and b) epoxy, MV (o.5 wt%), P25 (5 wt%) and alcohol (5 wt%).*

Next, our original alcohol, isopropanol, is compared to 1-phenethyl alcohol (Figure 2.7), showing that the reaction induction time is shorter with 1-phenethyl alcohol than with isopropanol. In summary, a more substituted alcohol leads to a faster reaction: 1-phenethyl alcohol, a highly substituted alcohol performs better than isopropanol. Therefore, 1-phenethyl alcohol will be used in the majority of the following experiments presented here.

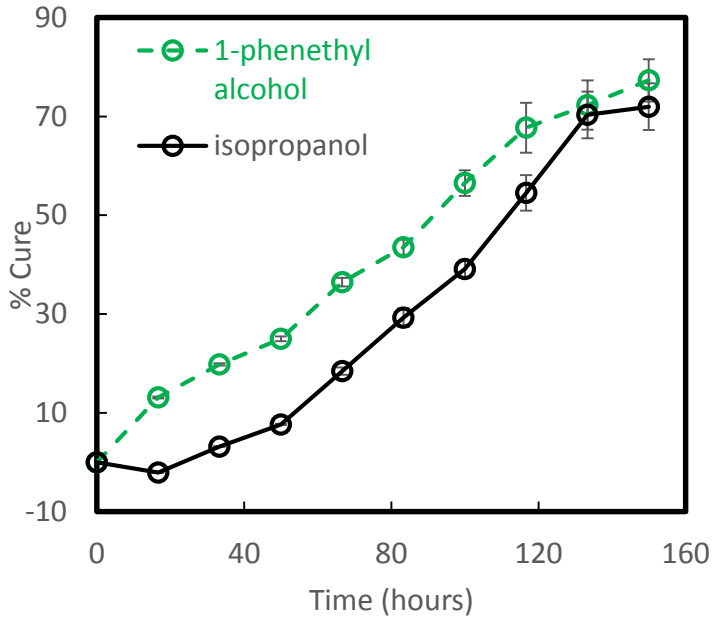


*Figure 2-7:* ***Effect of type of alcohol on cure.*** *Systems contain epoxy, MV (0.5 wt%), P25 (5 wt%) and alcohol: isopropanol (5 wt%) or 1-phenethyl alcohol at the same alcohol to epoxy molar ratio (10 wt%).*

Parametric study of system composition

Next, the effect of concentration of alcohol, MV and nanoparticles is systematically studied. The results are presented in Figure 2.8 where the effects of MV, alcohol and nanoparticle content are shown in (a), (b) and (c) respectively.

The curing rate depends non-monotonically on MV content with the highest rate occurring at 1 wt% MV. It is interesting to note how much more sensitive the curing rate is to MV content when the alcohol is 1-phenethyl alcohol (Figure 2.8a) than when it is isopropanol (Figure 2.6a), which indicates that second order effects that may be interesting to study in more detail. The non-monotonic behavior indicates that MV has both a positive and a negative effect on rate. The

positive effect is the electron scavenging which increases proton production. The negative effect could be the simple dilution effect which makes it less likely that two epoxide groups will meet. More investigation is required to adequately understand this.

The curing rate increases nonlinearly as alcohol content increases, at least within the range studied (1 to 10 wt%, Figure 2.8b). The rate increase occurs because the proton production rate depends directly on alcohol concentration although this effect appears to be dependent on quantum efficiency and system composition and thus limited.

While a higher nanoparticle (P25) content, and thus higher surface area, leads to a faster reaction, the increase is surprisingly little (Figure 2.8c), likely indicating that, in this system, surface area may not be the most important limiting factor.

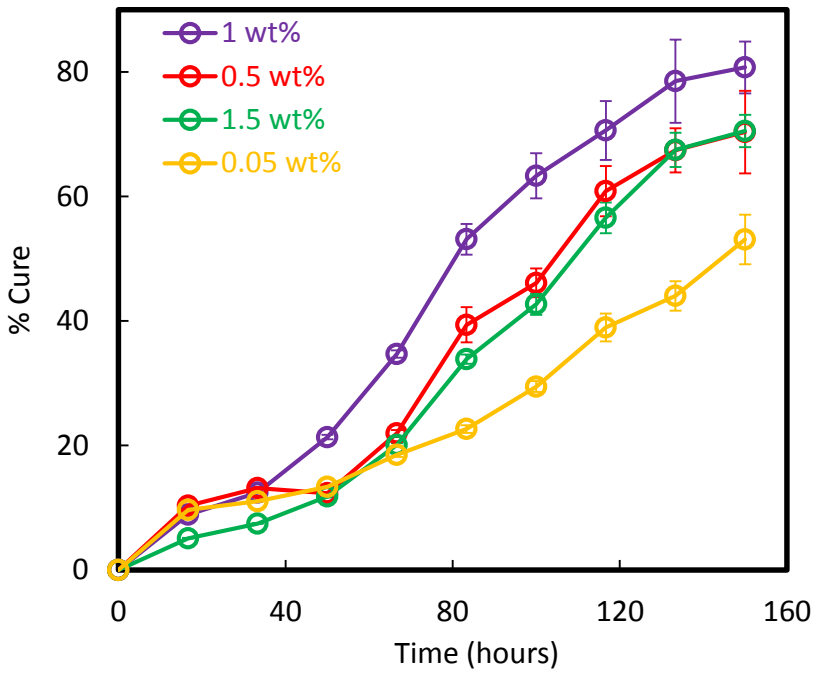
1 wt%
0.5 wt%
1.5 wt%
0.05 wt%
% Cure
Time (hours)
0
20
40
60
80
0
40
80
120
160

**(a)**

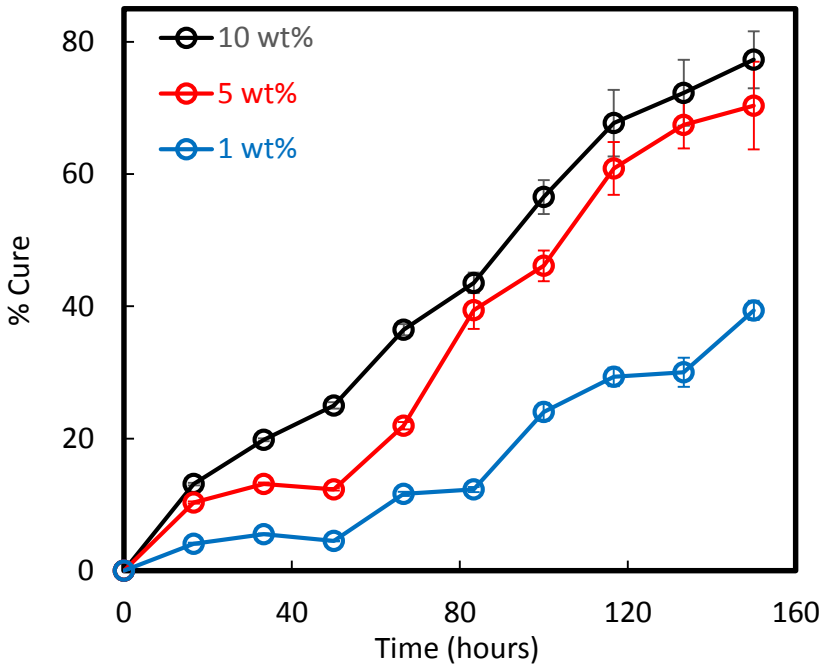
10 wt%
5 wt%
1 wt%
% Cure
Time (hours)
0
20
40
60
80
0
40
80
120
160

**(b)**

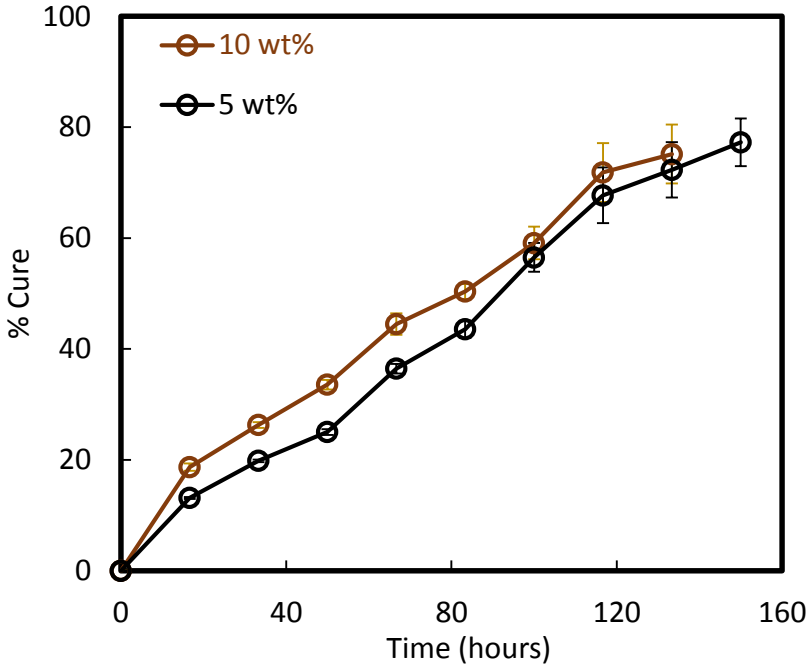


**(c)**

*Figure 2-8:* ***Effect of system composition on cure.*** *Systems contain a) epoxy, 1-phenethyl alcohol (5 wt%), P25 (5 wt%) and various concentrations of MV, b) epoxy, MV (0.5 wt%), P25 (5 wt%) and various concentrations of 1-phenethyl alcohol, and c) epoxy, MV (0.5 wt%), 1-phenethyl alcohol (10 wt%) and two concentrations of P25.*

Effect of nanoparticle crystal structure and size

Figure 2.9 shows the effect of nano particle crystal structure on curing at constant particle size and specific area. P25 contains both anatase and rutile crystals while the other nanoparticle is pure anatase. Not surprisingly, P25, which is known to be a very good photo catalyst[35] results in faster curing than pure anatase. The two crystal structures, anatase and rutile, have different energy levels and when the two are combined, one of the structures behaves as an electron scavenger for the other. Although, this is a predictable result, the experiment is necessary to benchmark the

performance of pure anatase because commercially available $TiO_2$ quantum dots are pure anatase. Crystallinity is also a factor which is likely to have an effect. Highly crystalline particles are devoid of structural defects. These defects act as recombination sites for photogenerated carriers. Due to the difficulty of accessing to TiO2 particles with same size but different crystallinity, the influence of crystallinity on photo-curing will not be treated here.

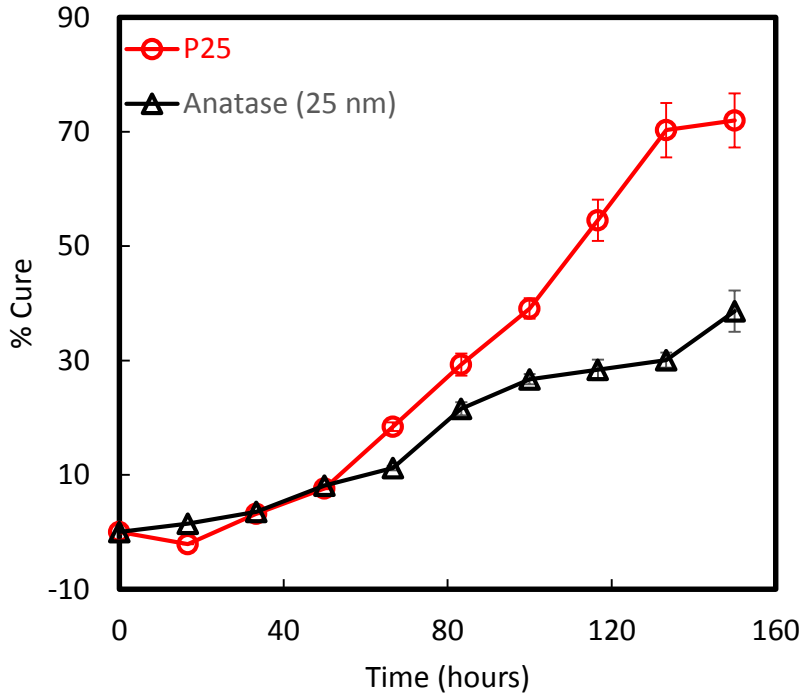


*Figure 2-9:* ***Effect of $TiO_2$ nanoparticle crystal structure on cure.*** *Systems contain epoxy, MV (0.5 wt%), isopropanol (5 wt%) and nanoparticles (5 wt%).*

Next, we consider the effect of $TiO_2$ anatase nanoparticle size at constant wt % and at constant surface area, Figure 2.10 a and b respectively. $TiO_2$ particles are known to exhibit quantized effects when smaller than 10 nm. Note that a different particle size will inevitably lead to different total surface area when the weight percentage is constant and that a constant surface area can only be achieved at different weight percentages.

In Figure 2.10a, curing is observed in both systems containing bulk or quantized $TiO_2$ nanoparticles. Both 5 nm and 10 nm particles lead to a faster reaction than the 25 nm particles because of the surface area effect. Systems containing 10 nm particles have a faster reaction than those containing 5 nm quantum dots, despite the smaller surface area, likely due to the blue shift

in the absorbance wavelength (248 nm) of the 5 nm particles away from the peak emittance of the 365 nm UV lamp. This can be compared to the 10 nm and 25 nm particles with absorbances at 264 nm and 260 nm respectively.

The bigger 25nm particles must be at 25 wt% to reach the same surface area as 5 wt% of the 10 nm particles. The reaction rate obtained for the system containing the 25 nm particles having the higher weight percentage is significantly higher than that of the system containing the smaller particles (Figure 2.10b). This indicates that the weight percentage of particles is the most important parameter in terms of rate of reaction and it may simply be a mass effect. It is curious, however, that when weight percentage of P25 is doubled (Figure 2.8c), the effect is not as significant. This poses many questions that are still open with regards to electron scavenging and significant second order effects.

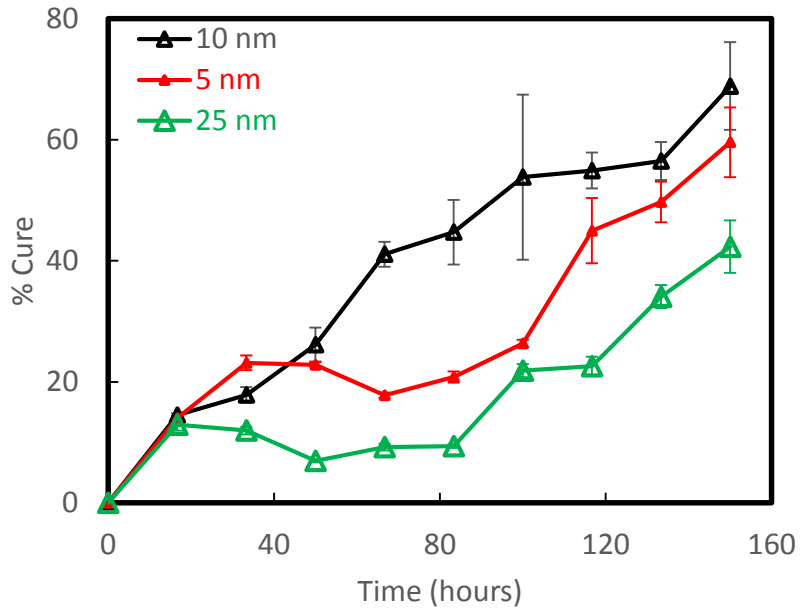


**(a)**

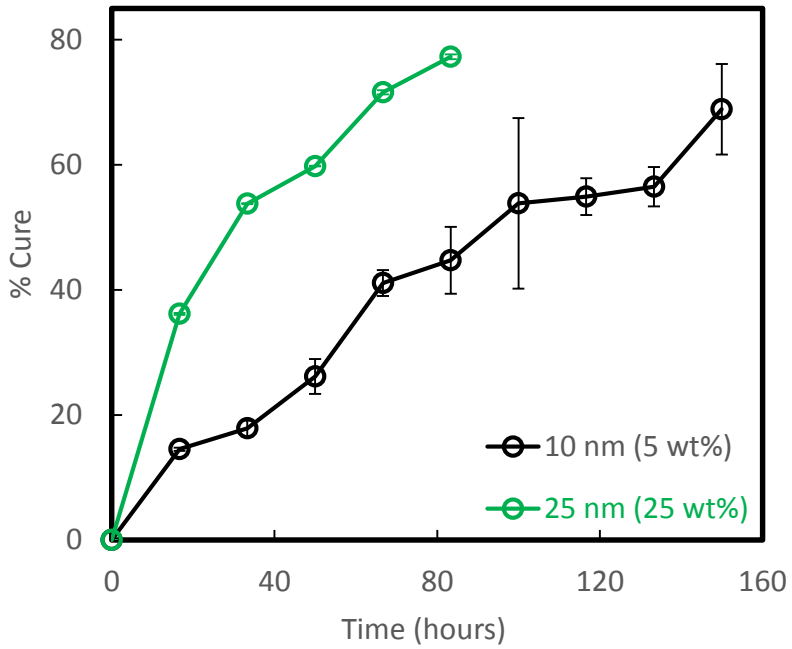


**(b)**

*Figure 2-10: **Effect of particle size on cure** at a) constant wt% (5 wt%), and b) constant surface area (12.75 $m^2$/g sample). Systems contain epoxy, 1-penylethanol (10 wt%), MV (0.5 wt%) and*

*anatase $TiO_2$. In (a) the total surface area per gram of mixture are 17.8, 12.75 and 2.5 $m^2$/gram with particles of size 5, 10 and 25 nm respectively.*

Best combination

Figure 2.11 shows the performance of the system with the best combination of parameters found in these studies and compares it to that of the original mixture used to verify the reaction mechanism. The best combination consists of 1 wt% MV, 10 wt% 1-phenethyl alcohol and 25 wt% of 10 nm anatase $TiO_2$ and reaches 65% cure in 33 h while the original mixture requires 150 h. This is an improvement of almost a factor of 5.

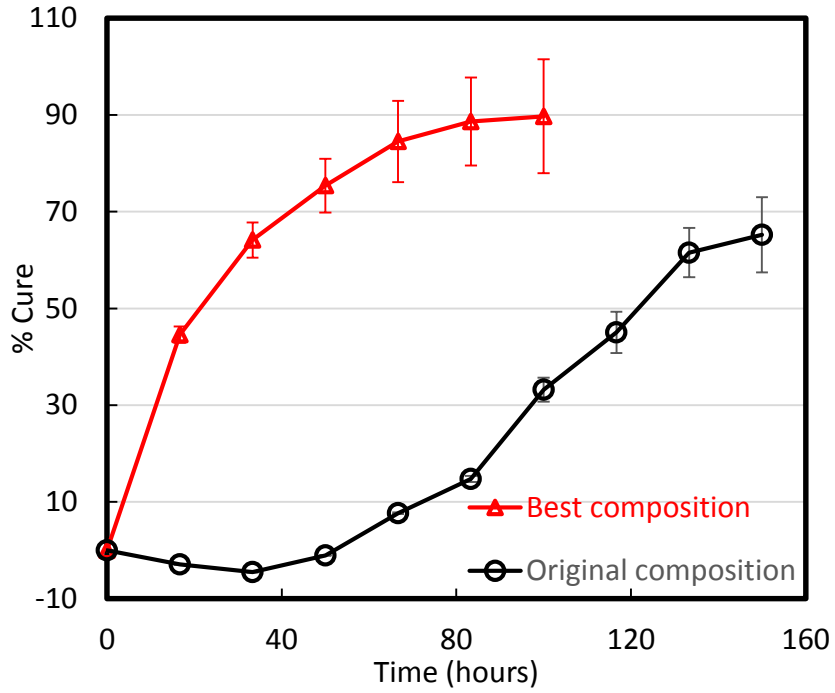


*Figure 2-11:* ***Curing behavior of the best system composition compared to that of the original.*** *The best composition is epoxy, 1-phenethyl alcohol (10 wt%), anatase TiO2 10nm (25 wt%) and MV (1 wt%). The original composition is epoxy, isopropanol (5 wt%) and P25 (5 wt%).*

## Conclusion

For the first time, we demonstrate that semiconducting nanoparticles can initiate epoxy photocuring. The reaction is observed by FTIR and titration and the proposed mechanism is supported by FTIR (C=O bands). The incorporation of an electron scavenger and an alcohol with

more substituted carbons increase the rate of reaction further supporting the proposed mechanism. A mixed crystal $TiO_2$ (anatase and rutile), P25, has superior catalytic performance compared to anatase titania of the same particle size and surface area. Surface area is an important factor, however, weight percentage of particles has a much more significant effect when comparing systems with the same surface area. This work is the critical first step in the development of tunable photoinitiators for epoxy curing that will allow the production of photostable products.

# 3. References


1. Black J T, Ronald A K, and DeGarmo E P. "Manufacturing and production systems." *DeGarmo's Materials and Processes in Manufacturing*. Hoboken, NJ: Wiley, 2008. Print.
2. Liou F W. "Modeling and virtual prototyping." *Rapid Prototyping and Engineering Applications: a Toolbox for Prototype Development*. Boca Raton: CRC, 2008. Print.
3. Horvath J. "Making a 3D model." *Mastering 3D printing.* A press, 2014: 33-46. Web.
4. Thompson R. *Prototyping and low-volume production.* London: Thames & Hudson, 2011. Print.
5. Murphy S V, and Atala A. "3D bioprinting of tissues and organs". *Nature Biotechnology*. 2014; 32: 773-785.
6. Petrovic V , Gonzalez J V H, Ferrando O J, Gordillo J D, Puchades J R B, and Grinan L P. "Additive layered manufacturing: sectors of industrial application shown through case studies." *International Journal of Production Research.* 2011; 49: 1061-1079.
7. "GE aviation executive, Greg Morris, honored for groundbreaking work in 3D printing". General Electric Aviation press release, 6 Mar. 2015. [Online] (Accessed 24 Aug. 2015). http://www.geaviation.com/press/services/services_20150306.html.
8. Harwood W, (2014, Oct. 6). *SpaceX launches dragon cargo ship to station* [Online] (Accessed 24 Aug. 2015). http://www.cbsnews.com/news/spacex-launches-space-station-cargo-ship/
9. Cesaretti G, Dini E, Kestelier X, Colla V, and Pambaguian L. "Building components for an outpost on the lunar soil by means of a novel 3D printing technology". *Acta Astronautica.* 2014; 93: 430-450.
10. Chand S. "Carbon fibers for composites". *Journal of material Science*. 2000; 35: 1303-1313.
11. Guo S, Yang X, Heuzey M, and Therriault D. "3D printing of a multifunctional nanocomposite helical liquid sensor". *Nanoscale*; 7: 6451-6456.
12. Hare C H. "The degradation of coatings by ultraviolet light and electromagnetic radiation". *The Journal of Protective Coating & Linings*; 1992; 5: 58-66.

13. Peiffer R W. “Applications of photopolymer technology”. *Photopolymerization Fundamentals and Applications*. Washington, DC: American Chemical Society. 1997: 1-14. Web.
14. Leubner W G, Albert S C, and Unruh C C. "Light-sensitive polymers for making Printing plates". Eastman Kodac Co, assignee. Patent US2861058. 18 Nov. 1958.
15. Barraud J, Gervat S, Ratovelmanana V, Boutevin B, Parisi J, Cahuzac A, and Jocteur R. "Polymer material of the polyurethane acrylate type for coating an optical fiber or for an optical fiber tape". Alcatel Cable, assignee. Patent US5567794. 22 Oct. 1996.
16. Crivello J. “The discovery and development of onium salt cationic photoinitiators.” *Journal of Polymer Science: Part A: Polymer Chemistry*. 1999; 37: 4241-4254.
17. Yagci Y, Jockusch S, and Turro N J. "Photoinitiated polymerization: advances, challenges, and opportunities". *Macromolecules*. 2010; 43: 6245-260.
18. Morseli D, Bondioli F, Sangermano M, and Messori M. “Photo-cured epoxy networks reinforced with $TiO_2$ in-situ generated by means of non-hydrolytic sol-gel process.” *Polymer*. 2012; 53: 283-290.
19. Crepeau P C, and Licari J J. "Electromagnetic radiation polymerization". North American Aviation Inc, assignee. Patent US3205157. 13 Sep 1965.
20. Xiao P, Zhang J, Dumur F, Tehfe M A, Morlet-Savary F, Graff B, Gigmes D, Fouassier J P, and Lalevee J. “Visible light sensitive photoinitiating systems: recent progress in cationic and radical photopolymerization reactions under soft conditions”. *Progress in Polymer Science*. 2015; 41: 32-66.
21. Hoffmann M R, Martin S T, Choi W, and Bahneman D W. "Environmental applications of semiconductor photocatalysis". *Chemical reviews*. 1995; 95: 69-96.
22. Kamat P V, Basheer R, and Fox M A. “Polymer-modified electrodes. Electrochemical and photoelectrochemical polymerization of 1-vinylpyrene”. *Macromolecules*. 1985; 18: 1366-1371.
23. Kuriacose J C, and Markham M C. “Mechanism of the photo-initiated polymerization of methyl methacrylate at zinc oxide surfaces”. *The Journal of Physical Chemistry*. 1961; 65: 2232-2236.

24. Hoffman A J, Yee H, Mills G, and Hoffmann M R. “Photoinitiated polymerization of methyl methacrylate using Q-sized ZnO colloids”. *The Journal of Physical Chemistry*. 1992; 65: 5540-5546.
25. Stroyuk A I, Granchak V M, Korzhak A V, and Kuchmii S Y. “Photoinitiation of buthylmethacrylate polymerization by colloidal semiconductor nanoparticles”. *Journal of Photochemistry of Photobiology A: Chemistry*. 2004; 162: 339-351.
26. Alivisatos A P. “Semiconductor clusters, nanocrystals, and quantum dos”. *Science.* 1996; 271: 933-937.
27. Bera D, Qian L, Tseng T, and Holloway P H. “Quantum dots and their multimodal application: A review”. *Materials*. 2010; 3: 2260-2345.
28. Brus L E. “Electron-electron and electron-hole interactions in small semiconductor crystallites: the size dependence of the lowest excited electronic state”. *Journal of Chemical Physics.* 1984; 80: 4403-4409.
29. Brus L E. “A simple model for the ionization potential, electron affinity, and aqueous redox potentials of small semiconductor crystallites”. *Journal of Chemical Physics.* 1983; 79: 5566-5571.
30. Michalet X, Pinaud F F, Bentolila L A, Tsay J M, Doose S, Sundaresan G, Wu A M, Gambhir S S, Weiss S. “Quantum dots for live cells, in vivo imaging, and diagnostics”. *Science*. 2005; 307: 538-544.
31. Gao X, Cui Y, Levenson R M, Chung L W K, and Nie S. “In vivo cancer targeting and imaging with semiconductor quantum dots”. *Nature biotechnology*. 2004; 22: 969-976.
32. Fujishima A, and Honda K. Electrochemical photolysis of water at a semiconductor electrode. *Nature*. 1972; 238: 37-38.
33. Chuang C M, Brown P R, Bulovic V, and Bawendi M G. “Improved performance and stability in quantum dot solar cells through band alignment engineering”. *Nature materials*. 2014; 13: 796-801.
34. Wood A, Glersig M, and Mulvaney P. “Fermi level equilibration in quantum dot-metal nanojunctions”. *Journal of Physical Chemistry B*. 2001; 105: 8810-8815.
35. Hurum D C, Agrios A G, and Gray K A. “Explaining the enhanced photocatalytic activity of Degussa P25 mixed-phase TiO2 using EPR”. *Journal of Physical Chemistry B*. 2003; 107: 4545-4549.

# 4. Conclusion and Future Work

The technology of 3D printing is the future of manufacturing. It is opening the door to many applications that not long ago could have only been science fiction. From 3D printing living organs using stem cells to 3D printing bases on the moon using lunar dust, it is opening new frontiers continuously. Its limitation is, as it often is, material development. For stereolithography 3D printing to be used in functional applications in aerospace or automotive applications, and replace the energy intensive and the poor quality of metal 3D printing, more photostable materials must be developed.

Stereolithography uses photocurable epoxy-based resins mixed with initiators, which absorb light at a specific wavelength and then produce protons that open up the epoxide rings so that they crosslink. Current catalysts are sensitive to UVA light that not only exists in the 3D printing laser but also in the solar spectrum on Earth, which renders the product unstable during its end use. Photocuring is revolutionizing our world via its critical role in 3D printing, coating, dentistry and PCB manufacturing. More research is needed to engineer different photocuring catalysts that respond to different wavelengths. In this research, catalysts sensitive exclusively to wavelengths below 300 nm are desired.

The ability of semiconducting materials to catalyze the photocuring of epoxy-based resins needed to be demonstrated first. Then the quantized effect can be used to tune the band gap energy of the semiconducting nanoparticles and their corresponding absorbance range to achieve the end goal. This same approach allows many advancements in LEDs, medical images and solar cell research. This research intertwines those three disciplines: the engineering of 3D printing, the chemistry of photocuring and the physics of quantum dots.

For the first time, we demonstrate that $TiO_2$ nanoparticles and quantum dots initiate the photocuring reaction of epoxy resins. A reaction mechanism is proposed where, after absorbing light of an energy corresponding to the band gap of the semiconductor, an exciton is formed. Then, the hole oxidizes an alcohol to a ketone, producing protons that ring-open epoxides leading to the crosslinking of the material.

Various parameters are investigated to improve the reaction kinetics. The use of an electron scavenger reduces the electron-hole recombination rate and reduces the induction time of the reaction. Using alcohol where the carbon carrying the OH group is more substituted leads to more stable intermediate radicals decreasing the induction time of the reaction. The concentration of the

catalyst, crystal structure and size (affecting band energy) all have significant effects on the reaction kinetics. The most influential factor is the weight percentage of the catalyst.

The results and implications of this study constitute a solid stepping stone towards exciting future studies. The next step in this research is to synthesize quantum dots that absorb only below 300 nm. Following that, it must be demonstrated that those quantum dots can cure epoxy-based resins only if light below 300 nm is used and that solar light triggers no curing. A complete evaluation of material photostability at this point is necessary. Further, the reaction kinetics and mechanical properties of the cured material must be significantly improved and optimized, possibly by studying second order effects. A photo-DSC will prove to be instrumental in further investigating the exact mechanism of the reaction.

Finally, compatibility of this new class of materials with stereolithography 3D printing must be investigated. A Stereolithography 3D printing of parts using this material must be demonstrated. Material compatibility with the process depends on many factors depending on the application: viscosity, cost, safety, smell, and taste. The ease of processing during printing and of dispersing the nanoparticles during material preparation depend on the viscosity but comes at the cost of mechanical properties. Most SLA material range between 165 and 2500 cP (the viscosity of the epoxy used at this study is 75 cP but formulation can change). The new cost and safety considerations stem from the use of nanoparticles instead of cationic initiators. While cost may increase, so will the utility (revenue) as the process no longer is used only to make models that are thrown away but also to make lasting parts that can be sold. The safety can be assessed once the material and type of quantum dots used are decided as not all nanoparticles fall under one category in terms of safety. Smell and taste are important if the product constantly interact with consumers such as children and will be a function of final formulation.

# 5. Appendices

## Appendix 1 : Controls

Figure 4.1 shows the UV-VIS spectra of the anatase nanoparticles used in suspension, with normalized absorbance. It shows a very slight shift in absorbance of the 5 nm particles (peak absorbance is at 248 nm) compared to those of the 10 and 25 nm particles (peak absorbance at 260 nm in both cases). In higher wavelengths, the absorbance observed is due to scattering.

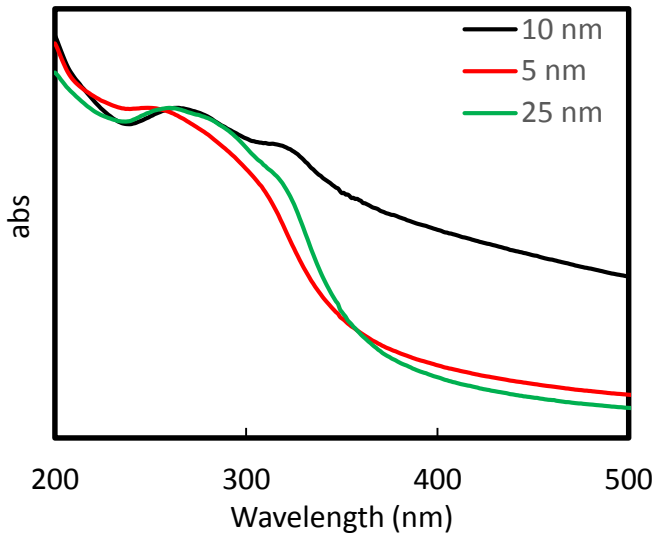


*Figure 4-1:* ***UV-VIS absorbance of anatase $TiO_2$ nanoparticles*** *of the indicated sizes showing a blue shift with the 5nm particles.*

Figure 4.2 shows the FTIR spectra of systems shown in Figure 2.3 before any irradiation showing that there is little difference and consequently validating the comparison in Figure 2.3.

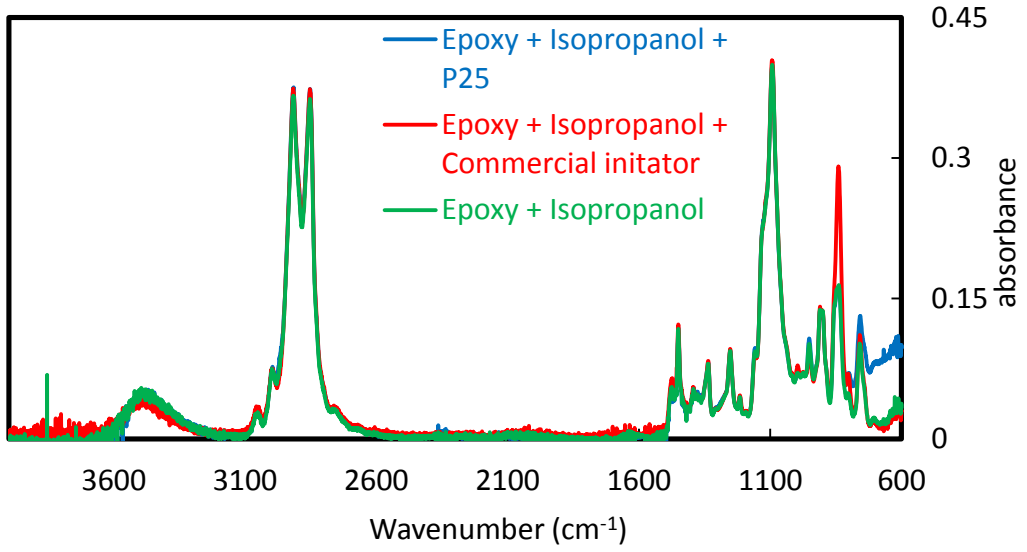


*Figure 4-2: **FTIR spectroscopy at t=0** from different systems shown in Figure 2.3*

Figure 4.3 shows controls without nanoparticles of the systems shown in Figure 2.6 showing that the do not exhibit any significant cure.

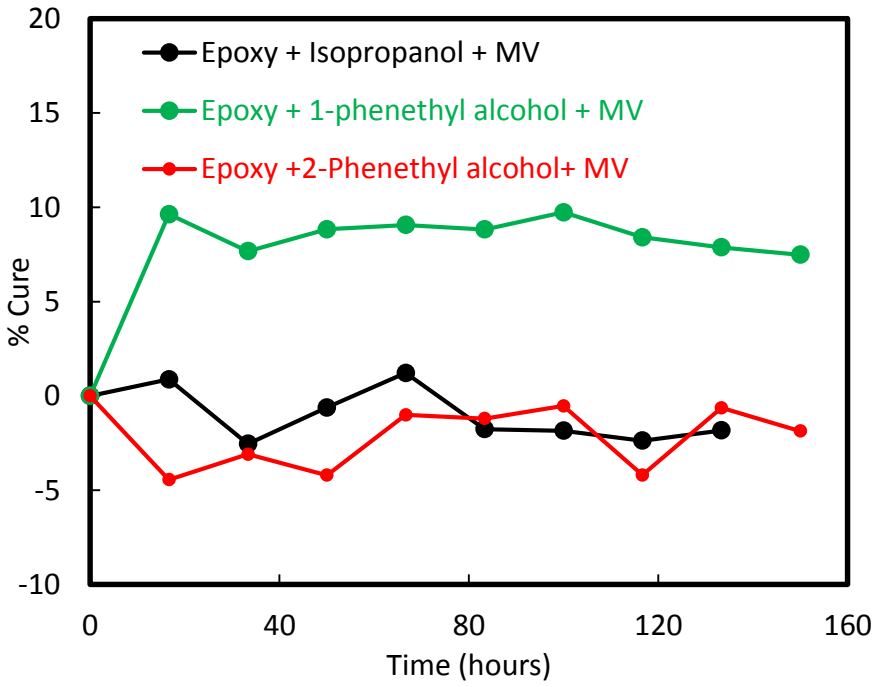


*Figure 4-3: **Controls without nanoparticles** of systems shown in Figure 2.6.*

## Appendix 2: Some second order effects

Effect of electron scavenger with bulk anatase

Figure 4-4 shows the effect of using an electron scavenger when the catalyst is 25nm anatase as opposed to P25 in Figure 2.6a. The use of MV improves performance in the system with 25 nm anatase which is consistent with what is observed with P25 in Figure 2.6a. However, the significance of that effect seem to be much higher with 25 nm anatase. This may indicate that electron-hole recombination in 25 nm anatase is more of a problem, mitigated by the use of the electron scavenger, in 25nm anatase than it is in P25 which is consistent with the principles behind P25 being a good catalyst.[35]

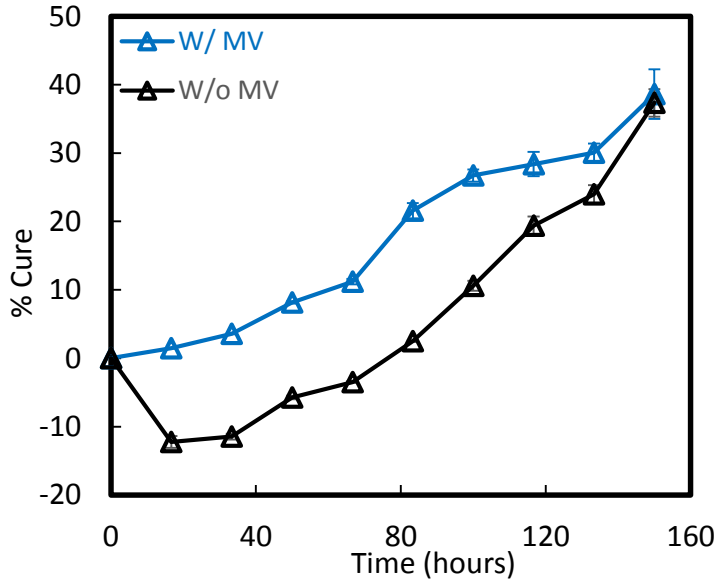


*Figure 4-4: **Effect of MV on cure when anatase nanoparticles used**. Systems contain epoxy, isopropanol (5 wt%) and $TiO_2$ (Anatase-25nm) (5 wt%). MV (0.5 wt%) is added to one kind of the samples as indicated*

Effect of the alcohol with bulk anatase

Figure 4-5 shows the effect of using 1-phenethyl alcohol as the alcohol as opposed to using isopropanol when 25 nm anatase is used as opposed to P25 Figure 2.7. The improvement due to the use of the alcohol with the more substituted carbon, is very unclear in Figure 4.4 as opposed to how it is in Figure 2.7. The reaction still starts much earlier when 1-phenethyl alcohol is used. However, that advantage seem to be eroding away as time passes. The reasons behind that are

unclear and more investigations are needed. A detailed parametric study of second order effect is compelled by those observations. Furthermore, analysis of the system from energy levels and physical chemistry point of view is also necessary to understand the factors in play.

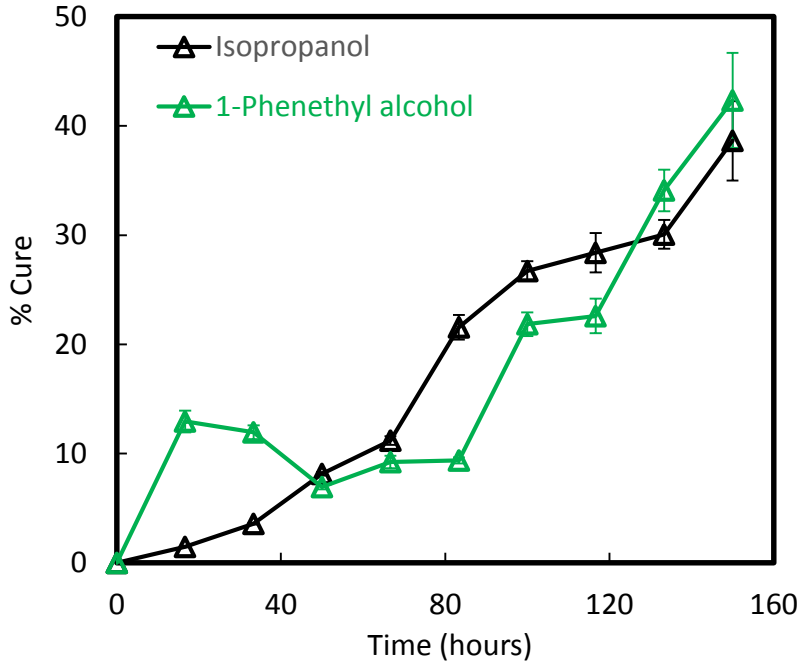


*Figure 4-5:* ***Effect of alcohol on cure when anatase nanoparticles are used.*** *Systems contain epoxy, MV (0.5 wt%), $TiO_2$ (Anatase-25 nm) (5 wt%) and alcohol: isopropanol (5 wt%) or 1-phenethyl alcohol with the same molar ratio as when isopropanol is used (10 wt%).*